

พอลิไดแอเซทิลีนจากไดแอเซทิลีนลิพิดที่มีหมู่ไฮลิโกเอทิลีนไกลคอลเพื่อเป็นเซ็นเซอร์วัดอุณหภูมิและ
ไอออนโลหะ

นายพัฒน์ นาควิบูลย์วงศ์

วิทยานิพนธ์นี้เป็นส่วนหนึ่งของการศึกษาตามหลักสูตรปริญญาวิทยาศาสตรมหาบัณฑิต

สาขาวิชาปิโตรเคมีและวิทยาศาสตร์พอลิเมอร์

คณะวิทยาศาสตร์ จุฬาลงกรณ์มหาวิทยาลัย

ปีการศึกษา 2553

ลิขสิทธิ์ของจุฬาลงกรณ์มหาวิทยาลัย

POLYDIACETYLENE FROM DIACETYLENE LIPIDS CONTAINING
OLIGO(ETHYLENE GLYCOL) AS THERMAL AND
METAL ION SENSORS

Mr. Pat Narkwiboonwong

A Thesis Submitted in Partial Fulfillment of the Requirements
for the Degree of Master of Science Program in Petrochemistry and Polymer Science
Faculty of Science
Chulalongkorn University
Academic Year 2010
Copyright of Chulalongkorn University

Thesis Title POLYDIACETYLENE FROM DIACETYLENE LIPIDS
 CONTAINNING OLIGO(ETHYLENE GLYCOL) AS
 THERMAL AND METAL ION SENSORS
By Mr.Pat Narkwiboonwong
Field of Study Petrochemistry and Polymer Science
Thesis Advisor Associate Professor Mongkol Sukwattanasinitt, Ph.D.

Accepted by the Faculty of Science, Chulalongkorn University in Partial
Fulfillment of the Requirements for the Master's Degree

.....Dean of the Faculty of Science
(Professor Supot Hannongbua,Dr.rer.nat.)

THESIS COMMITTEE

.....Chairman
(Assistant Professor Warinthorn Chavasiri, Ph.D.)

.....Thesis Advisor
(Associate Professor Mongkol Sukwattanasinitt, Ph.D.)

.....Examiner
(Associate Professor Voravee Hoven, Ph.D.)

.....External Examiner
(Gamolwan Tumcharern, Ph.D.)

พัฒนา นาควิบูลย์วงศ์ : พอลิไดอะเซทิลีนจากไดอะเซทิลีนลิพิดที่มีหมู่โอลิโกเอทิลีนไกลคอล เพื่อเป็นเซ็นเซอร์วัดอุณหภูมิและไอออนโลหะ (POLYDIACETYLENE FROM DIACETYLENE LIPIDS CONTAINING OLIGO(ETHYLENE GLYCOL) AS THERMAL AND METAL ION SENSORS)

อ.ที่ปรึกษาวิทยานิพนธ์หลัก: รศ.ดร.มงคล สุขวัฒนาสินิทธิ, 68 หน้า.

อนุพันธ์เอสเทอร์ของ 10, 12-pentacosadiynoic acid (PCDA) 3 ชนิด และเอไมด์ 1 ชนิด ได้สังเคราะห์ขึ้นเพื่อใช้เป็นตัวปรับสมบัติของพอลิ PCDA เช่นเซอร์ ไดอะเซทิลีนลิพิดเอสเทอร์เตรียมได้จากปฏิกิริยาเอสเทอริฟิเคชันระหว่าง 10, 12-pentacosadiynoic acid (PCDA) กับเอทิลีนไกลคอลได้ EG-PCDA, ไตรเอทิลีนไกลคอลได้ 3EG-PCDA และ เพนทอะเอทิลีนไกลคอลได้ 5EG-PCDA โดยมีกรดเป็นตัวเร่งปฏิกิริยา ส่วนอนุพันธ์เอไมด์ของไดอะเซทิลีนนั้นเตรียมผ่านปฏิกิริยาควบแน่นระหว่างเมทิลเอสเทอร์ของ PCDA กับเอทานอลามีน (NEG-PCDA) ไดอะเซทิลีนลิพิดผสมระหว่าง PCDA และอนุพันธ์ที่สังเคราะห์ขึ้นสามารถกระจายตัวในน้ำได้โดยกระบวนการอัลตราโซนิเคชันได้โซลของคอลลอยด์โปร่งแสง เมื่อได้รับแสงอัลตราไวโอเล็ตสามารถเกิดโฟโตพอลิเมอไรเซชันเป็นพอลิไดอะเซทิลีน (PDA) สีน้ำเงิน การเปลี่ยนสีตามอุณหภูมิจากน้ำเงินเป็นแดงของโซล PDA ติดตามได้โดยการวัดค่าการดูดกลืนแสงของพอลิไดอะเซทิลีนสีแดงที่ความยาวคลื่น 540 นาโนเมตร ในช่วงอุณหภูมิ 20-80 องศาเซลเซียส ด้วยเครื่องยูวี-วิส สเปกโทรมิเตอร์ การพลอตอนุพันธ์อันดับที่หนึ่งของค่าการดูดกลืนเทียบกับอุณหภูมิ (dA/dT) พบว่าพอลิไดอะเซทิลีนที่มีส่วนผสมของไดอะเซทิลีน เอสเทอร์แสดงการเปลี่ยนแปลงสีสองช่วงอุณหภูมิโดยความว่องไวในการเปลี่ยนสีช่วงแรกนั้นแปรผันตามความยาวของสายโอลิโกเอทิลีนไกลคอล ส่วนการเปลี่ยนสีในช่วงที่สองนั้นสอดคล้องกับการเปลี่ยนแปลงสีของ poly(PCDA) ที่อุณหภูมิ 65 องศาเซลเซียส ในขณะที่พอลิไดอะเซทิลีนลิพิดผสม NEG-PCDA แสดงการเปลี่ยนแปลงสีแบบต่อเนื่องขั้นตอนเดียว ในการทดสอบพอลิไดอะเซทิลีนที่มีไดอะเซทิลีนเอสเทอร์ 30% โมล สำหรับการตรวจวัดพบไอออนโลหะหนัก เช่น Cd^{2+} , Co^{2+} , Cu^{2+} , Fe^{2+} , Hg^{2+} , Ni^{2+} , Pb^{2+} และ Zn^{2+} พบว่ามีเพียงไอออนของตะกั่ว (Pb^{2+}) เท่านั้นที่ทำให้พอลิไดอะเซทิลีนที่มี 5EG-PCDA/PCDA เป็นส่วนผสมเปลี่ยนจากสีน้ำเงินเป็นแดงอย่างชัดเจน โดยมีความสามารถตรวจวัดได้ต่ำสุดที่ 10 μM หรือ 2 ppm

สาขาวิชา ปี โตรเคมีและวิทยาศาสตร์พอลิเมอร์ ลายมือชื่อนิสิต.....
ปีการศึกษา 2553..... ลายมือชื่อ อ.ที่ปรึกษาวิทยานิพนธ์หลัก.....

5072386523: MAJOR PETROCHEMISTRY AND POLYMER SCIENCE

KEYWORDS: POLYDIACETYLENE/ THERMOCHROMISM/ ETHYLENE GLYCOL

PAT NARKWIBOONWONG: POLYDIACETYLENE FROM DIACETYLENE LIPIDS CONTAINING OLIGO(ETHYLENE GLYCOL) AS THERMAL AND METAL ION SENSORS. THESIS ADVISOR: ASSOC. PROF. MONGKOL SUKWATTANASINITT, 68 pp.

Three ethylene glycol esters and one ethanolamide derivatives of 10,12-pentacosadiynoic acid (PCDA) were synthesized and studied as a modulator for poly(PCDA) sensor. Ethylene glycol (EG-PCDA), triethylene glycol (3EG-PCDA) and pentaethylene glycol esters (5EG-PCDA) were synthesized by simple acid catalyzed esterification of PCDA with ethylene glycol and the corresponding oligo(ethylene glycol). The preparation of the amide derivative, NEG-PCDA, was performed via a condensation between the methyl ester of PCDA and ethanolamine. The mixed lipids between PCDA and its derivative can be dispersed in milli-Q water by ultrasonication, giving translucent sol. After being irradiated with UV light, the mixed lipid sols undergo photopolymerization to generate the desired blue polydiacetylene (PDA) sols. The blue to red thermochromic transition of PDA sols were monitored by observing the absorbance of the red phase of PDA at 540 nm in the range of 20-80 °C using temperature variable UV-vis spectrometer. The derivative (dA/dT) plot of the PDA sols containing diacetylene esters showed two steps of color transition while the PDA sol containing diacetylene amide exhibited continuous one-stepped color transition. In the two-stepped color transition, the second step observed around 65 °C associated with the color transition temperature of poly(PCDA). The PDA sols containing 30% mole of the diacetylene esters were assessed for colorimetric detection of heavy metal ions such as Cd^{2+} , Co^{2+} , Cu^{2+} , Fe^{2+} , Hg^{2+} , Ni^{2+} , Pb^{2+} and Zn^{2+} . At 100 μM , only Pb^{2+} caused a distinct color change of the sol from blue to red for the PDA sol of 5EG-PCDA/PCDA mixed lipid. The sol showed the detection limit of Pb^{2+} as low as 10 μM (~2 ppm).

Field of Study: Petrochemistry and Polymer Science Student's Signature:

Academic Year: 2010..... Advisor's Signature:

ACKNOWLEDGEMENTS

I would like to express my sincere gratitude to my advisor, Associate Professor Mongkol Sukwattanasinitt, Ph.D., for his invaluable guidance, excellent and kind supervision, and helpful suggestion throughout this research. This thesis research would not be completed without his advice and guidance.

My appreciation is also given to Assistant Professor Warinthorn Chavasiri, Ph.D. and Associate Professor Voravee Hoven, Ph.D., thesis defense committee, for their kind attention, valuable suggestion and recommendations. I also would like to thank Associate Professor Tirayut Vilaivan, Ph.D., for permission to use UV-Vis spectrophotometer throughout this research.

I would like to thank Gamolwan Tumcharern, Ph.D., thesis defense committee from National Nanotechnology Center (NANOTEC).

I would like to thank Center for Petroleum, Petrochemicals and Advanced Materials

Furthermore, I gratefully thank to my friends at dormitory for their genuine, help, and friendship and everyone in MS-group, especially Dr, Anupat Potisatityuenyong for training; Miss Jasuma, Miss Sansanee and Mr. Theodtoon for their educated, suggestion and big help in everything. Moreover, I express my appreciation to Warathip, Nakorn, Thirawat, Chaiwat, Thanakrit and for spirit, smile, good wish and their helps in everything.

Finally, I would like to express thankfulness to my family for their love, care, encouragement and support throughout my study.

CONTENTS

	Page
Abstract (Thai)	iv
Abstract (English)	v
Acknowledgements	vi
Contents	vii
List of Figures	ix
List of Schemes	xiii
List of Abbreviations	xiv
CHAPTER I INTRODUCTION	1
1.1 Polydiacetylene.....	1
1.1.1 Polydiacetylene vesicles.....	1
1.1.2 Optical and electronic properties of PDA.....	2
1.1.3 Chromism properties.....	4
1.2 Interaction of metal ion with functionalized lipid membrane.....	11
1.3 Oligo Ethylene glycol.....	15
1.4 Lead ion(Pb^{2+}).....	17
1.5 Objectives and scope of thesis.....	24
CHAPTER II EXPERIMENTAL	25
2.1 Synthetic procedures.....	26
2.1.1 Synthesis of EG-PCDA, 3EG-PCDA, 5EG-PCDA.....	25
2.1.2. Synthesis of amido derivative (NEG-PCDA).....	28
2.2 Preparation of polydiacetylene (PDA) sols.....	29
2.3 Study of thermochromism.....	30

	Page
2.4 Study of colorimetric responses of the PDA sols to metal ions.....	30
CHAPTER III RESULTS AND DISCUSSION.....	31
3.1 Synthesis of glycol-modified PCDA derivatives.....	31
3.2 Preparation of diacetylene sols and their polymerization.....	34
3.3 Thermochromism of mixed lipid PDA sols	36
3.4 Development of metal ion sensor from polydiacetylene mixed vesicles.....	42
CHAPTER IV CONCLUSION	48
4.1 Conclusion.....	48
REFERENCES.....	49
APPENDICES.....	57
Appendix A.....	58
Appendix B.....	62
Appendix C.....	64
VITAE.....	68

LIST OF FIGURES

Figure	Page
1.1 Packing parameters: $r = 5 \text{ \AA}$ and $\Phi = \sim 45^\circ$ required for the topological polymerization of a diacetylene monomer.....	1
1.2 Structure and formation of a PDA vesicle from a diacetylene lipid.....	2
1.3 Color of polydiacetylene gel obtained from the odd and even diacetylene Monomer.....	3
1.4 Thermochromic reversibility of PCDA-mBzA showing a) absorption spectra during heating, b) cooling and c) intramolecular hydrogen bonding between the side chains of PCDA-mBzA.....	5
1.5 Polydiacetylene nanofiber gels with thermochromic reversibility between purple and red colors.....	5
1.6 Thermochromic reversibility of polydiacetylene blended with poly(vinyl pyrrolidone)	6
1.7 Proposed side-chain movement in the chromic transitions of poly(PCDA) vesicles.....	7
1.8 a) synthesis of amide diacetylene lipid monomers. b) Color of PDA sols recorded by photography during the heating process displaying the variation of color transition temperature.....	8
1.9 Picture of a well plate containing: valinomycin/PC/PDA and Monensin/PC/PDA solutions after addition of ions.....	9
1.10 Titration of the ion selective cation sensor with alkaline ion.....	10
1.11 Schematic representation of the G-quadruplex formation and the resulting steric repulsion.....	10
1.12 Crown six ether modified lipid with pyrene fluorophore.....	12
1.13 Illustration of the dispersion of initially aggregated receptor-lipids in a phospholipid membrane upon metal ion recognition.....	13
1.14 TEM image of a self-assembled, columnar structured lipid bilayer stack that forms after Cu^{2+} addition.....	14

Figure	page
1.15 The phase transition on temperature Maleic anhydride styrene grafted with oligo ethylene glycol.....	15
1.16 Synthesis of water soluble polystyrene.....	16
1.17 structure of hyperbranched polyether.....	16
1.18 The fluorescence emission spectrum of the probe dns-ECEE shift upon addition of Pb^{2+}	18
1.19 Schematics of DNAzyme-directed assembly of gold nanoparticles.....	18
1.20 Kinetics of nanoparticle aggregation in the presence of different Pb^{2+} concentrations.....	19
1.21 Mechanism for the Fluorescent Change of sensor after addition of Pb^{2+}	20
1.22 Schematic of the DNAzyme-Based Electrochemical Sensor.....	21
1.23 Shown are alternating current voltammograms of the sensor obtained after 1 h incubation at various Pb^{2+} concentrations.....	21
1.24 A redox, chromogenic and fluorescent chemosensor molecule.....	21
1.25 Schematic of crown-annelated thethiophenes complex with Pb^{2+}	22
1.26 Schematic of utilizing Pb^{2+} -induced allosteric G-quadruplex DNAzyme.....	23
3.1 1H -NMR spectrum of EG-PCDA, 3EG-PCDA and 5EG-PCDA in $CDCl_3$	33
3.2 1H -NMR spectrum of NEG-PCDA in $CDCl_3$	34
3.3 Color photographs mixed diacetylene lipid.....	35
3.4 Thermochromism photographs of EG-PCDA/PCDA.....	36
3.5 Thermochromism photographs of 3EG-PCDA/PCDA.....	36
3.6 Thermochromism photographs of 5EG-PCDA/PCDA.....	37
3.7 Thermochromism photographs of NEG-PCDA/PCDA.....	37
3.8 Temperature dependence of the absorpbance (A) at 540 nm of the mixed lipid sols.....	38
3. 9 First transition temperature of EG-PCDA/PCDA, 3EG-PCDA/PCDA and 5EG-PCDA/PCDA.....	39
3.10 Proposed assemblies of EG-PCDA, 3EG-PCDA, 5EG-PCDA/PCDA mixed lipids.....	41

Figure	Page
3.11 Colorimetric responses (%CR) of the mixed lipid PDA sols containing 30% mole of EG-PCDA, 3EG-PCDA and 5EG-PCDA.....	43
3.12 Colorimetric responses (%CR) to Pb^{2+} (100 μ M) of PDA sols prepared from NEG-PCDA.....	44
3.13 AFM images of PDA vesicles obtained from air dry samples of 5EG-PCDA/PCDA.....	45
3.14 Colorimetric responses (%CR) to various concentration Pb^{2+} and Zn^{2+} of the PDA sol.....	46
3.15 Colorimetric responses (%CR) to various metal ions (100 μ M) of the mixed lipid PDA sols of 5EG-PCDA/PCDA.....	47
A1 1H NMR; 2-hydroxyethyl pentacos- 10,12- diynoate (EG-PCDA).....	58
A2 1H NMR; 2-(2-(2 hydroxyethoxy) ethoxy) ethyl pentacos-10,12-diynoate (3EG-PCDA).....	58
A3 1H NMR; 14-hydroxy-3,6,9,12–tetraoxatetradecyl pentacos-10,12-diynoate (5EG-PCDA).....	59
A4 1H NMR; N-(2hydroxyethyl) pentacos-10,12-diynamide (NEG-PCDA)....	59
A5 13C NMR; 2-hydroxyethyl pentacos- 10,12- diynoate (EG-PCDA).....	60
A6 13C NMR; 2-(2-(2 hydroxyethoxy) ethoxy) ethyl pentacos-10,12-diynoate (3EG-PCDA).....	60
A7 13C NMR; 14-hydroxy-3,6,9,12–tetraoxatetradecyl pentacos-10,12-diynoate (5EG-PCDA).....	61
A8 13C NMR; N-(2hydroxyethyl) pentacos-10,12-diynamide (NEG-PCDA)...	61
B1 Mass spectra (ESI+) of EG-PCDA.....	62
B2 Mass spectra (ESI+) of 3EG-PCDA.....	62
B3 Mass spectra (ESI+) of 5EG-PCDA.....	63
B4 Mass spectra (ESI+) of NEG-PCDA.....	63
C1 Temperature dependence of the absorbance (A) at 540 nm of the mixed lipid sols EG-PCDA/PCDA.....	64
C2 Derivative plot (dA/dT) of mixed lipid sols EG-PCDA/PCDA.....	64

Figure	Page
C3 Temperature dependence of the absorbance (A) at 540 nm of the mixed lipid sols 3EG-PCDA/PCDA.....	65
C4 Derivative plot (dA/dT) of mixed lipid sols 3EG-PCDA/PCDA.....	65
C5 Temperature dependence of the absorbance (A) at 540 nm of the mixed lipid sols 5EG-PCDA/PCDA.....	66
C6 Derivative plot (dA/dT) of mixed lipid sols 5EG-PCDA/PCDA.....	66
C7 Temperature dependence of the absorbance (A) at 540 nm of the mixed lipid sols NEG-PCDA/PCDA.....	67
C8 Derivative plot (dA/dT) of mixed lipid sols NEG-PCDA/PCDA.....	67

LIST OF SCHEMES

	Page
Scheme 3.1 Synthesis of Three ethylene glycol esters and one ethanolamido derivatives of PCDA.....	32

LIST OF ABBREVIATIONS AND SIGNS

Abs	Absorbance
Å	Angstrom
AFM	Atomic force microscopy
cm	Centimeter
CR	Colorimetric response
CHCl ₃	Chloroform
CDCl ₃	Deuterated chloroform
°C	Degree celsius
g	Gram
mL	Millilitre
mM	Millimolar
nm	Nanometre
min	Minute
NMR	Nuclear magnetic resonance spectroscopy
ppm	Part per million
PDA	Polydiacetylene
PCDA	10,12-pentacosadiynoic acid
EG-PCDA	2-hydroxyethyl pentacos- 10, 12-diynoate
3EG-PCDA	2-(2-(2-hydroxyethoxy)ethoxy)ethyl pentacos-10,12-diynoate
5EG-PCDA	14-hydroxy-3,6,9,12-tetraoxatetradecyl pentacos-10,12 diynoate
NEG-PCDA	N-(2-hydroxyethyl)pentacos-10,12-diynamide
UV/vis	Ultra violet-visible
w/w	Weight by weight
λ	Wavelength
δ	Chemical shift
%	Percent

CHAPTER I

INTRODUCTION

1.1 Polydiacetylene

A polydiacetylene (PDA) is an ene-eye conjugated polymer consisting of double and triple bonds in its backbone. It can be prepared by topological 1,4 addition polymerization of a diacetylene monomer by heat, UV-light or γ rays.⁽¹⁻³⁾ PDAs possess several interesting chromic properties including their ability to change color by various stimuli such as heat, solvent and mechanical stress.

Topological polymerization of PDA requires suitable rather specific distance and orientation angle between diacetylene monomeric molecules within their condense phase packing. The polymerization occurs when the distance (r) between two monomers is around 5 Å and the orientation angle (θ) is $\sim 45^\circ$ relative to the translation axis (Figure 1.1).⁽⁴⁻⁵⁾

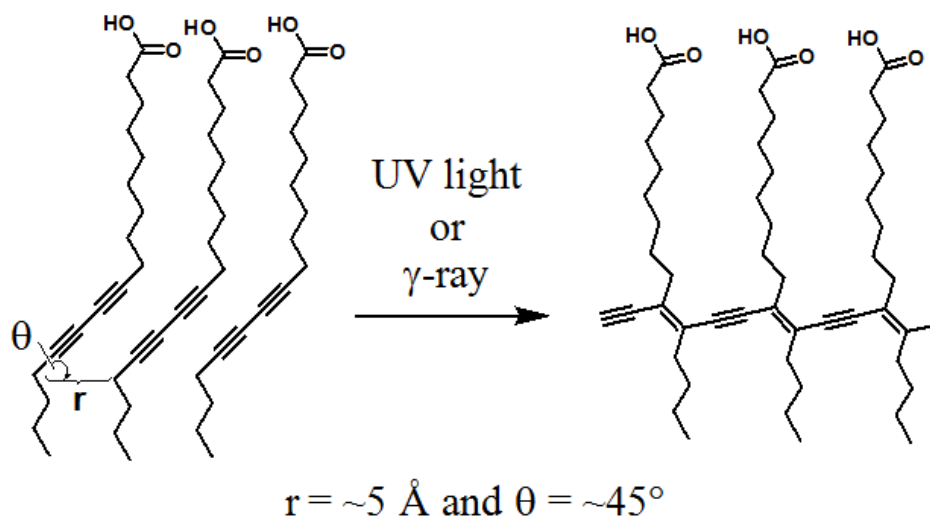


Figure 1.1 Packing parameters: $r = \sim 5 \text{ \AA}$ and $\theta = \sim 45^\circ$ required for the topological polymerization of a diacetylene monomer.

1.1.1 Polydiacetylene vesicles

PDAs can be prepared in a wide range of organized structures such as single crystal, Langmuir monolayer film, multilayer film, nano tube and vesicle. The vesicle is one of most widely used for application of PDA sensors. Vesicle is spherical assemble of lipids bilayer composing of hydrophobic parts concealed from water and hydrophilic head

groups faced to water. Several diacetylene lipids can self assemble into nano vesicles and polymerize into PDA provided that their topological packing orientations are allowed (Figure 1.2). One of the most studied diacetylene lipids is 10,12-pentacosadiynoic acid (PCDA) of which lipid vesicle has been mainly related to the development into bio-⁽⁶⁻¹⁴⁾ and chemosensors⁽¹⁵⁻¹⁹⁾.

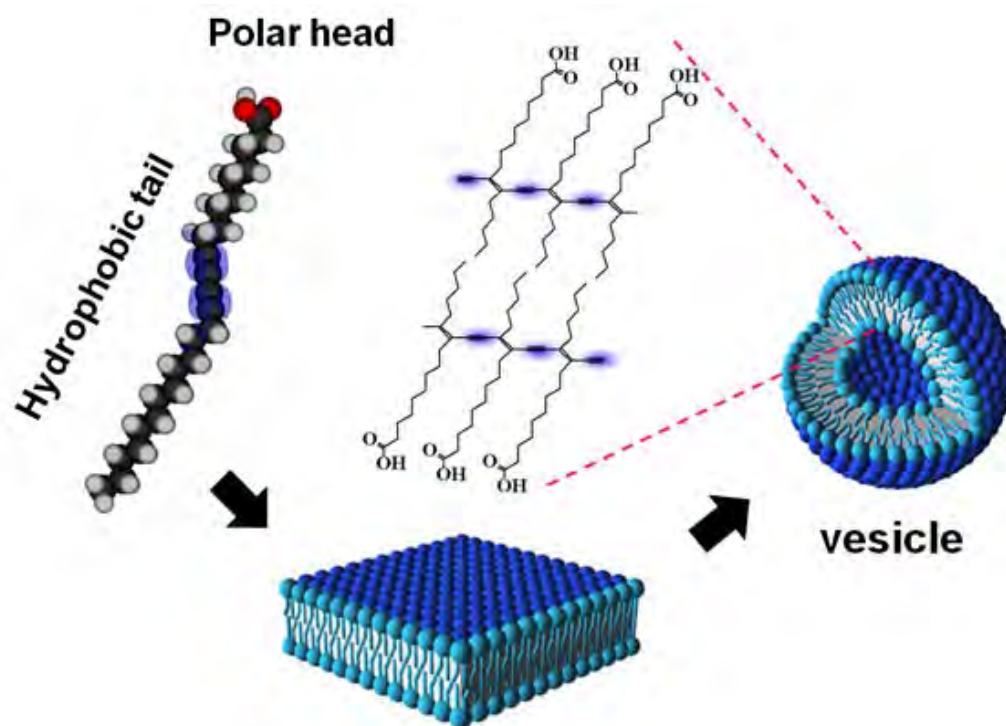


Figure 1.2 Structure and formation of a PDA vesicle from a diacetylene lipid.

1.1.2 Optical and electronic properties of PDA

Most diacetylene monomers are white or have no color but the color appears after polymerization due to ene-eye conjugated backbone of PDAs. The strong coupling between the electronic structure and the UV-visible absorption of PDAs led to their unique optical and electronic properties. Those properties demonstrated tremendous interests in this class of conjugated polymers. The blue color forms are most widely used for sensing applications. Usually, a blue PDA shows the maximum electronic absorption around 630-650 nm. Some PDAs are obtained in red color in which case the absorption maximum appeared at lower wavelength around 530-550 nm.⁽²⁰⁾ The electronic

absorption associates with the excitation energy of electron in a HOMO ground state to a LUMO excited state. It is thus possible to modify the electronic absorption spectrum of PDA by varying the degree of polymerization and steric factors of the substituents in the diyne monomer.⁽²¹⁻²²⁾ For example, Fujita, N. and coworker studied the relation of the number of the methylene side chain in bipolar (bolar) diacetylene amphiphilic monomers to the color of the resulting PDA gels in hexane (Figure 1.3).⁽²³⁾ The PDA exhibited blue color when the number of the methylene side chain was even but exhibited red color when the number was odd. They proposed the difference in bending angle of the polymer conjugated backbone induced by the packing of hydrogen bonded side chains of the “odd monomer” and “even monomer”. The higher bending angle of the polymer backbone obtained from the odd monomer produced a less conjugation which increased the band gap of the electronic states and thus the absorption energy.

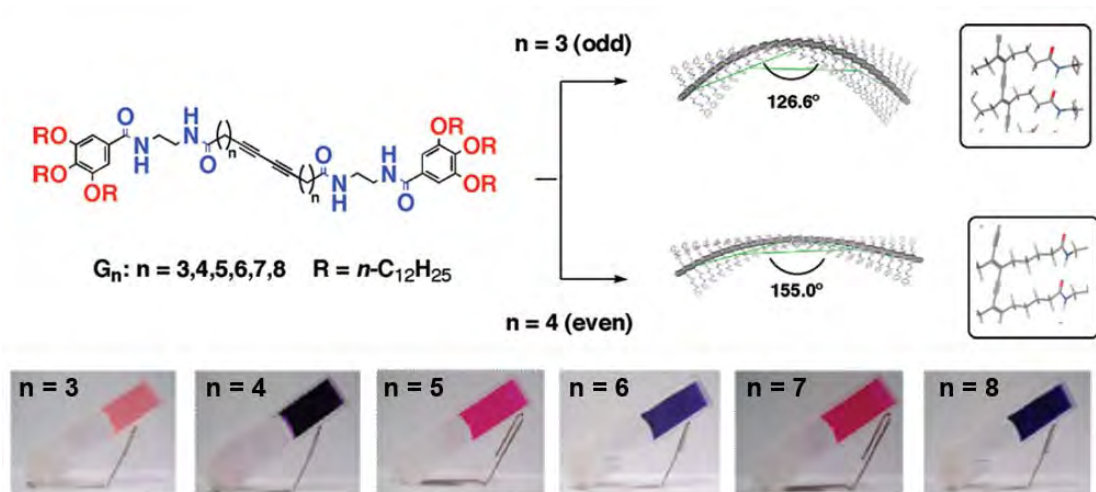


Figure 1.3 Color of polydiacetylene gel obtained from the odd and even diacetylene monomers.

1.1.3 Chromism properties

One of the most important properties of PDA is its ability to change color upon perturbation by external stimulant such heat, chemical, solvent and mechanical stress. The color change by heat called thermochromism.⁽²⁴⁻³¹⁾ The color change caused by

solvent called solvatochromism.⁽³²⁾ The color change caused by mechanical stress called mechanochromism.⁽³³⁾

A quantitative value for the extent of blue-to-red color transition is given by the colorimetric response (%CR) which is defined as

$$\%CR = (FB_0 - FB) / FB_0 \times 100$$

where FB is a blue fraction determined from $A_{\text{blue}} / (A_{\text{blue}} + A_{\text{red}})$. A_{blue} and A_{red} are the absorbance at the λ_{max} of the blue and red phases of the PDA, typically at 640 and 540 nm, respectively. FB_0 is the initial blue fraction before the PDAs are subjected to a concerned perturbation. The visible absorbance is measured by a UV-vis spectrometer.

Thermochromism

Thermochromism is the color transition when increase temperature which is one of the earliest known properties of PDAs. The thermochromic process can be either irreversible or reversible depended on side chain substituent and hydrogen bonding. Despite decades of research, the mechanism for color change has not yet been fully understood. Several reports have suggested that both side chain order and hydrogen bonding affected the color transition of PDAs. For example, Kim, J. and coworkers have reported relation between intramolecular hydrogen bonding between the side chains of PCDA-mBZA and the thermochromic reversibility (Figure1.4).⁽²⁷⁾

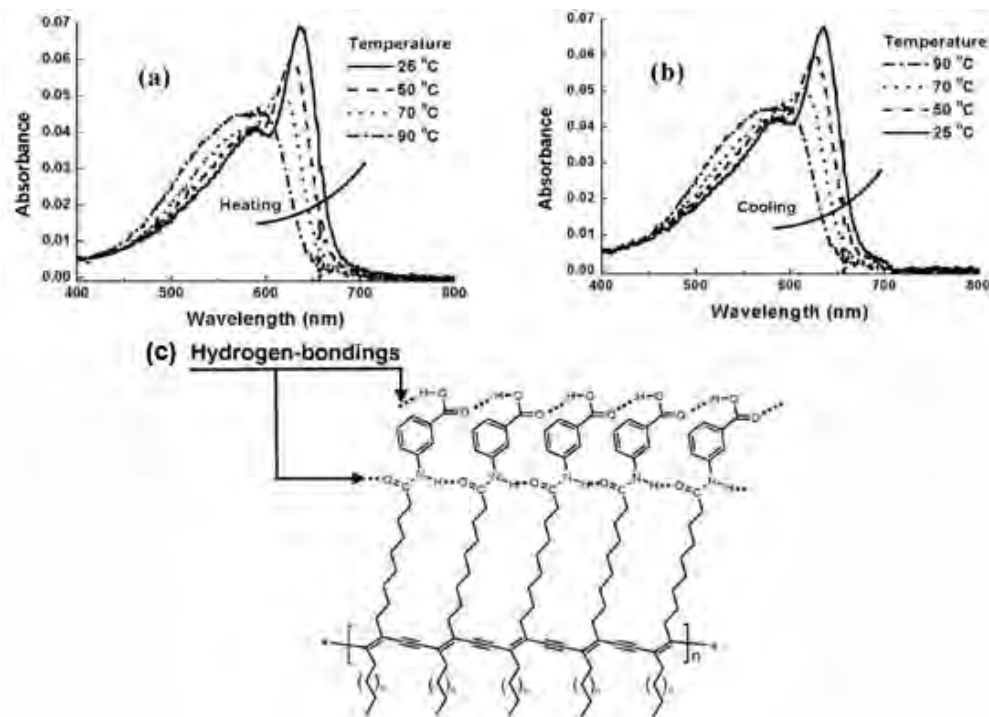


Figure 1.4 Thermochromic reversibility of PCDA-mBzA showing a) absorption spectra during heating, b) cooling and c) intramolecular hydrogen bonding between the side chains of PCDA-mBzA.⁽²⁷⁾

Dautel, O. J. and coworkers reported the thermochromic reversibility between purple and red colors of polydiacetylene nanofiber gels prepared from diacetylene monomers containing urea groups. Upon heating the interaction between two hydrogen bonds between the urea groups pattern have been broken that cannot go back to a constrained situation in the blue form after cooling producing a partially thermochromic reversibility (Figure 1.5).⁽²²⁾

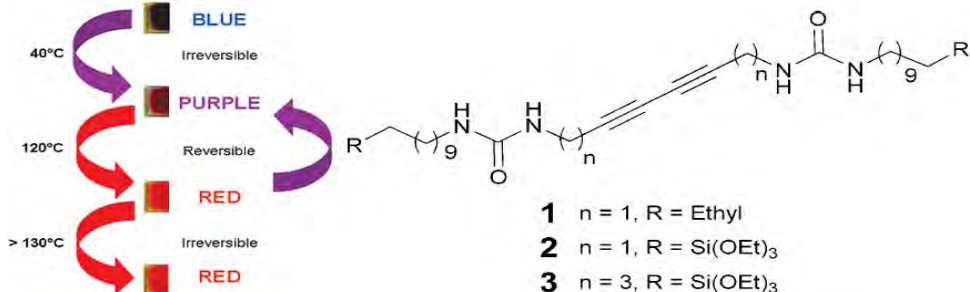


Figure 1.5 Polydiacetylene nanofiber gels with thermochromic reversibility between purple and red colors.⁽²²⁾

In 2008, Gu, Y. and coworkers investigated the blending product of nanocrystal of 10,12 pentacosadiynoic acid (PCDA) and poly(vinylpyrrolidone). The blending product had intermolecular hydrogen bonding between carboxylic head groups of PCDA with pyrrolidone groups that constituted thermochromic reversibility (Figure 1.6).⁽³⁴⁾

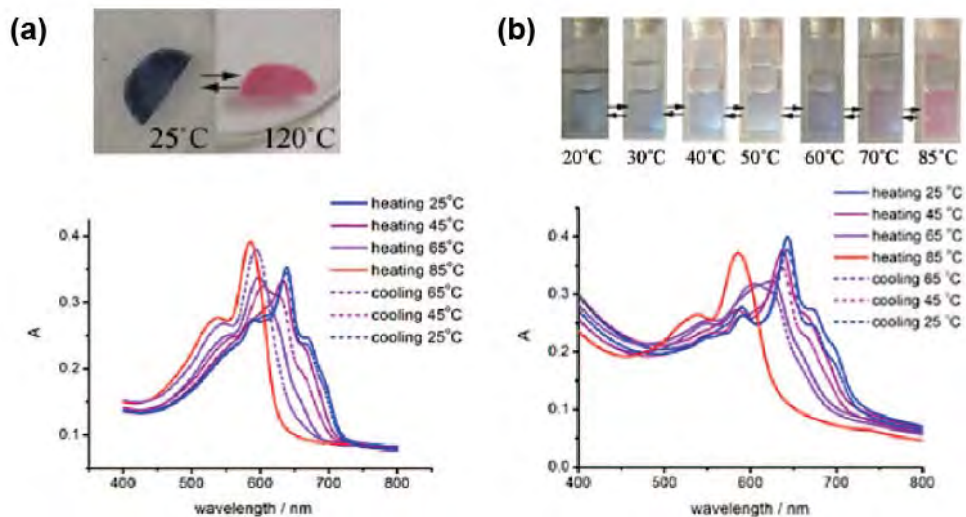


Figure 1.6 Thermochromic reversibility of polydiacetylene blended with poly(vinylpyrrolidone) a) polymer blend film, b) its aqueous suspension.⁽³⁴⁾

In 2008, Potisatityuenyong, A. and co workers conducted extensive investigation of chromic properties, i.e. thermochromism, solvatochromism and alkalinochromism of poly(PCDA) vesicle sol.⁽²⁴⁾ In the case of solvatochromism and alkalinochromism, UV-vis absorption show the similar pattern, blue to red color transformation. The decreasing and increasing in absorbance of red and blue phase, respectively, without peak shifting, indicated a quantitative conversion between the blue and red vesicles. Thermochromism was, however, different. The steady hypsochromic shift and color reversibility of the vesicle sol at low temperature were observed, indicating colorimetric reversibility. On the other hands, when heating over 75 °C the blue color was not recovered upon cooling. The mechanism proposed for solvatochromism and alkalinochromism is related to sudden hydrogen bond breaking by solvation or deprotonation processes while the mechanism proposed for thermochromism is involved gradual weakening of the hydrophobic interaction and hydrogen bond as shown in Figure 1.7.

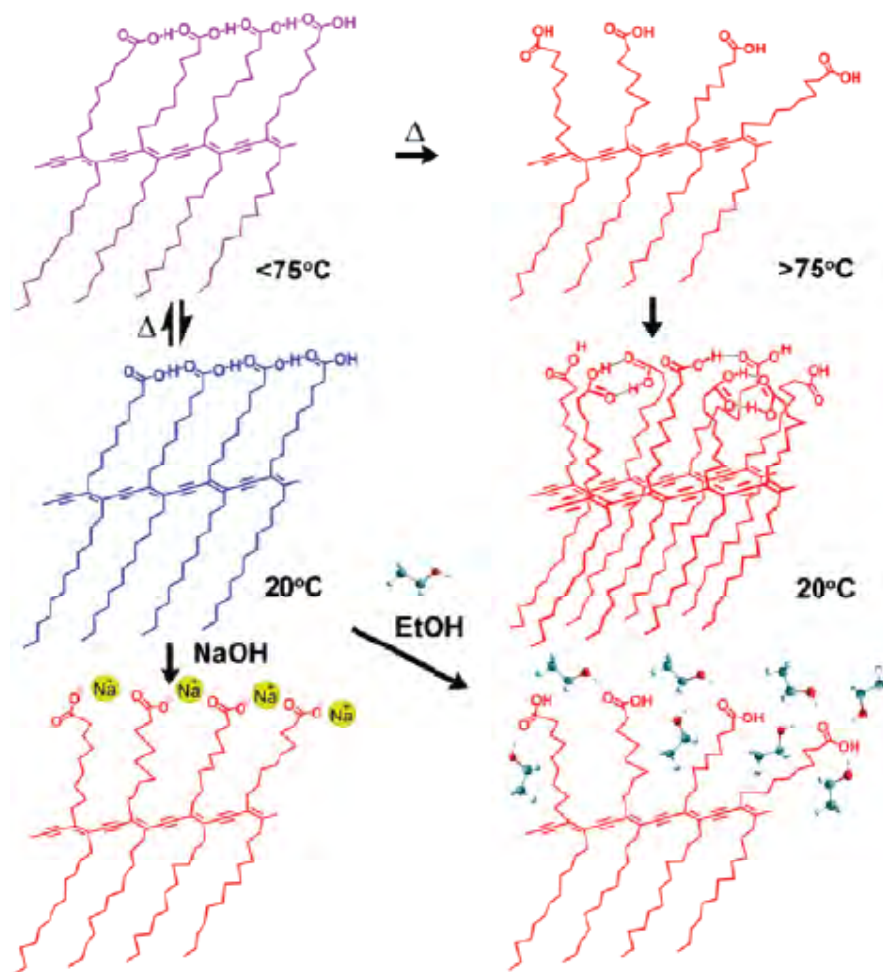


Figure 1.7 Proposed side-chain movement in the chromic transitions of poly(PCDA) vesicles.

In 2010, Wacharasindhu S. and co-workers have reported that PDA with tunable thermochromic reversibility could be obtained from amide derivatives of PCDA.⁽³⁵⁾ Mono- and diamide derivatives of PCDA were synthesized from condensation of PCDA with various aliphatic and aromatic diamines (Figure 1.8a). The PDA of the amido-PCDA derivatives were prepared by photopolymerization of their molecular assembly homogeneously dispersed in aqueous media. Thermochromic properties of the resulting PDA sols were studied by temperature variable UV-Vis spectrometry along with photographic recording. The color transition temperatures and thermochromic reversibility of the polymers are varied depended on the number of amide groups and the structure of aliphatic and aromatic linkers (Figure 1.8b). With phenylenediamide and polymethylenediamide linkers, the bisdiynamide PDA showed complete thermochromic

reversibility while the monoamide analogues were only partially reversible. The results provide a fundamental idea about the factors affecting the thermochromic properties of polydiacetylenes toward the development of materials for universal thermal indicators.

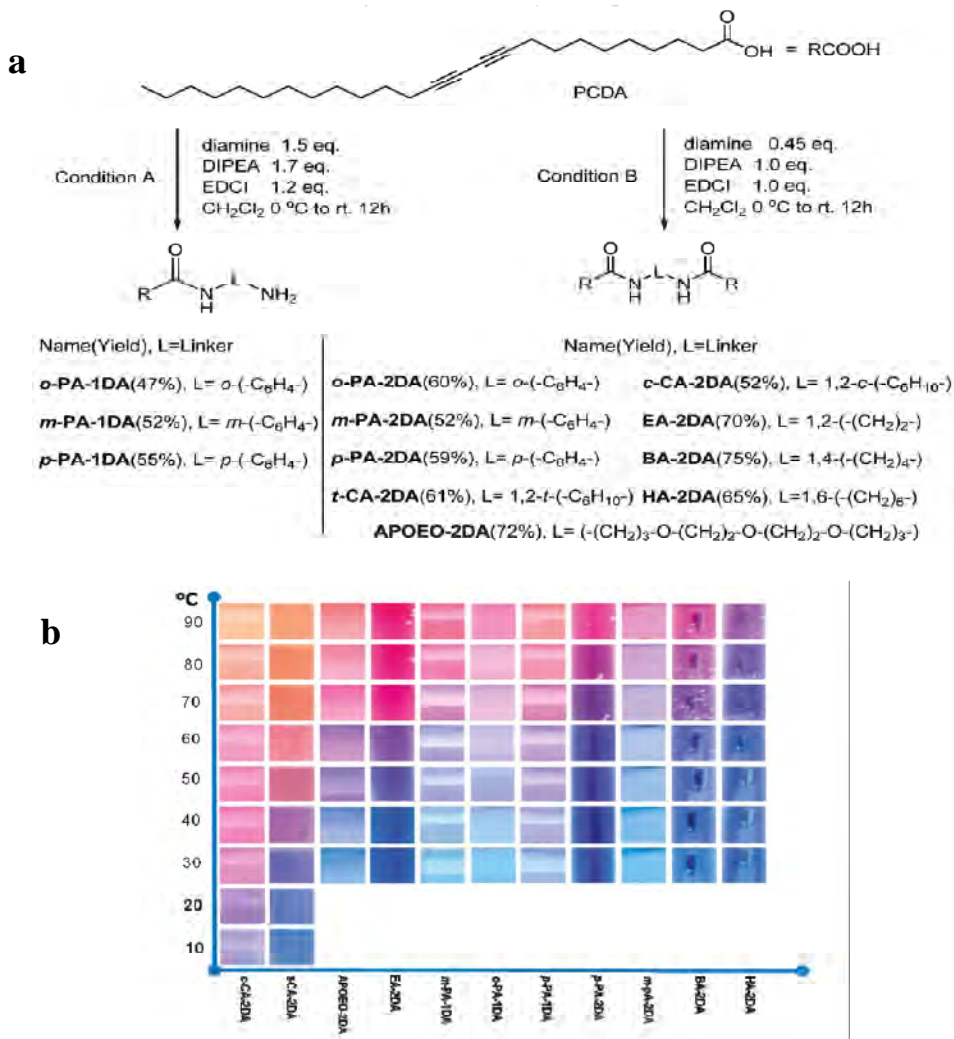


Figure 1.8 a) synthesis of amide diacetylene lipid monomers. b) Color of PDA sols recorded by photography during the heating process displaying the variation of color transition temperature.⁽³⁵⁾

Mechanochromism

Mechanochromism is a property where a material changes its color in response to an applied stress or strain. The blue-to-red transition of PDAs may be induced by some mechanical force. For example, Muller, H and Eckhardt C. J. observed an irreversible transition in a PDA single crystal induced by compressive stress, which resulted in

coexisting blue and red phases.⁽³⁶⁾ Nallicheri, R. A. and Rubner, M. F. observed reversible mechanochromism for conjugated PDA chains embedded in a host poly urethane elastomer that was subjected to tensile strain.⁽³³⁾

Chemochromism

Jelinek, R. and coworkers investigated a supramolecular assemblies of vesicles composed of ionophore and phospholipid (PC) embedded in polymerized diacetylene. The ionophore embedded PDA vesicle were shown to undergo color change from blue to red after additional of specific cation. The color transition of the vesicle is directly related to the binding of cations with the ionophore. For example, a bacteria ionophore namely valinomycin has a specific binding with $Rb^+ > K^+ > Cs^+$. After the addition of Rb^+ in a valinomycin embedded vesicle, the color of the vesicle changed from blue to red while the addition of Li^+ and Na^+ ion did not (Figure 1.9).⁽¹⁸⁾ Titration of the cation selective sensor showed a detection limit of less than 0.5 mM (Figure 1.10).

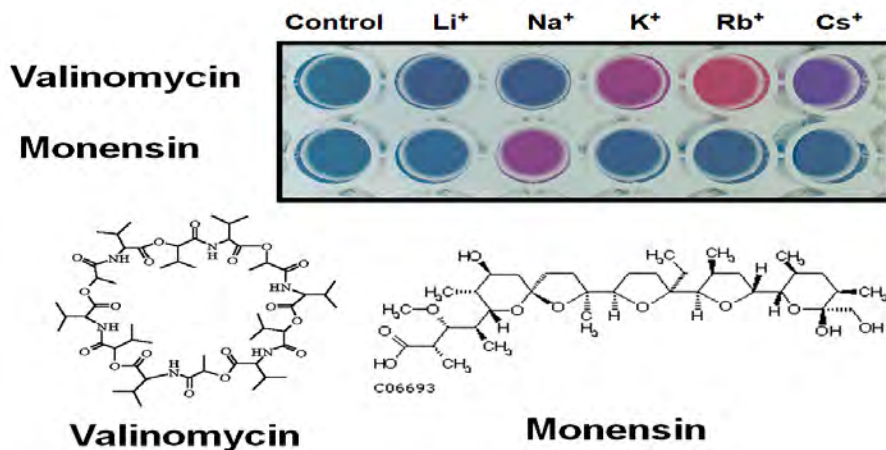


Figure 1.9 Picture of a well plate containing: valinomycin/PC/PDA and Monensin/PC/PDA solutions after addition of ions.⁽¹⁸⁾

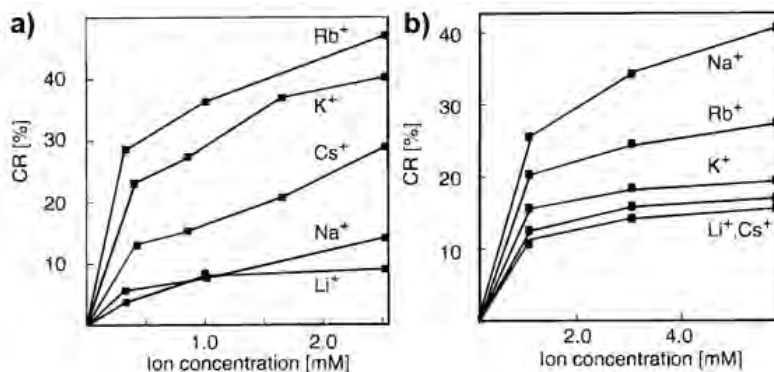


Figure 1.10 Titration of the ion selective cation sensor with alkaline ion, a) valinomycin/PC/PCDA, b) monensin/PC/PDA.⁽¹⁸⁾

In 2008 Lee, J. and coworkers have reported poly(PCDA) attached with G-rich ssDNA have been used for selective fluorometric detection of potassium ion induce by G-Quadruplex between K^+ and G-rich ssDNA (**Figure 1.11**).⁽³⁷⁾

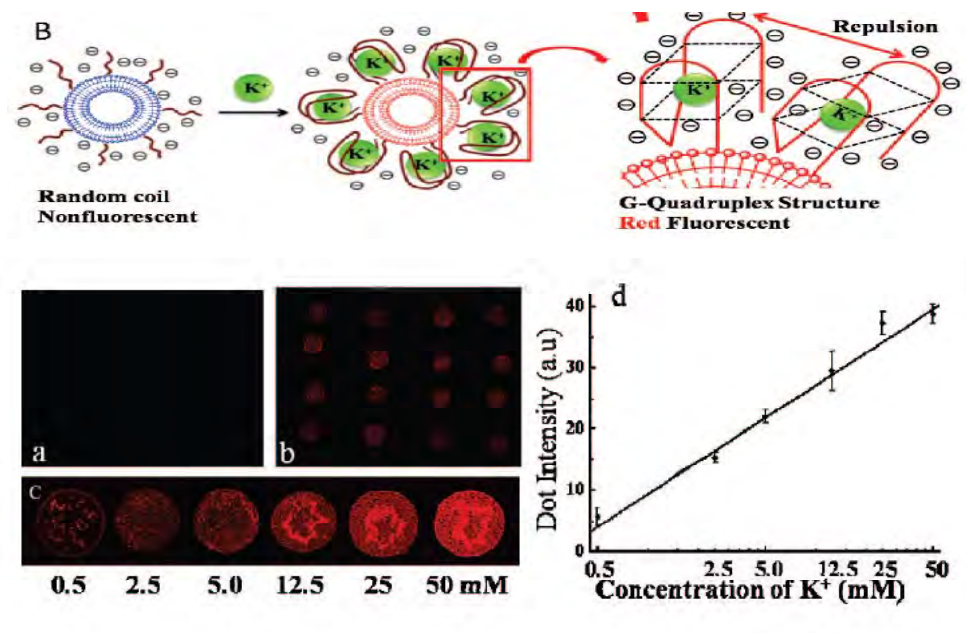


Figure 1.11 (Up) Schematic representation of the G-quadruplex formation and the resulting steric repulsion. **(Down)** Fluorescent microscope images of the microarrayed PDA liposomes (excitation at 600 nm and a long-pass emission filter with 550 nm cutoff were used) (a) after adding 5 mM NaCl (b) after adding the KCl solution in 30 min of incubation at room temperature. (c) Fluorescent images of the PDA liposome arrays with KCl solutions at various concentrations. (d) Correlation curve between the fluorescence intensity and the amount of the K^+ .⁽³⁷⁾

1.2 Interaction of metal ion with functionalized lipid membrane

Chemical recognition events on lipid membranes are the initiating steps toward cellular signaling. Particularly interesting are the recognition phenomena that occur with the cell membrane which pathogenic agents must be rapidly and precisely distinguished from innocuous agents. Although some lipids have complex functionality for recognition of specific ligands, even the simplest structures also selectively bind metal ions and ligand. Changes in the lipid's phase transition temperature and aggregational state in the

membrane can lead to marked changes in the membrane structure. The metal ion interaction with membrane can be exploited as metal ion sensor material.

In 2002, Sasaki, D.Y. and coworker studied an interaction of crown six ether modified lipid in phospholipid membrane with some heavy metal ion such as Zn^{2+} , Hg^{2+} and Pb^{2+} . A fluorophore, pyrene, was connected with crown ether lipid to use as a fluorescence probe (Figure 1.12 a). The results from fluorescence emission spectroscopy and AFM image indicated an aggregation of crown ether lipid on the phospholipid membrane. Recognition of lead ion by the crown ether cause the lipid's headgroup to become cationic resulting in electrostatic repulsion between Pb^{2+} bound lipid (Figure 1.12).⁽³⁸⁾

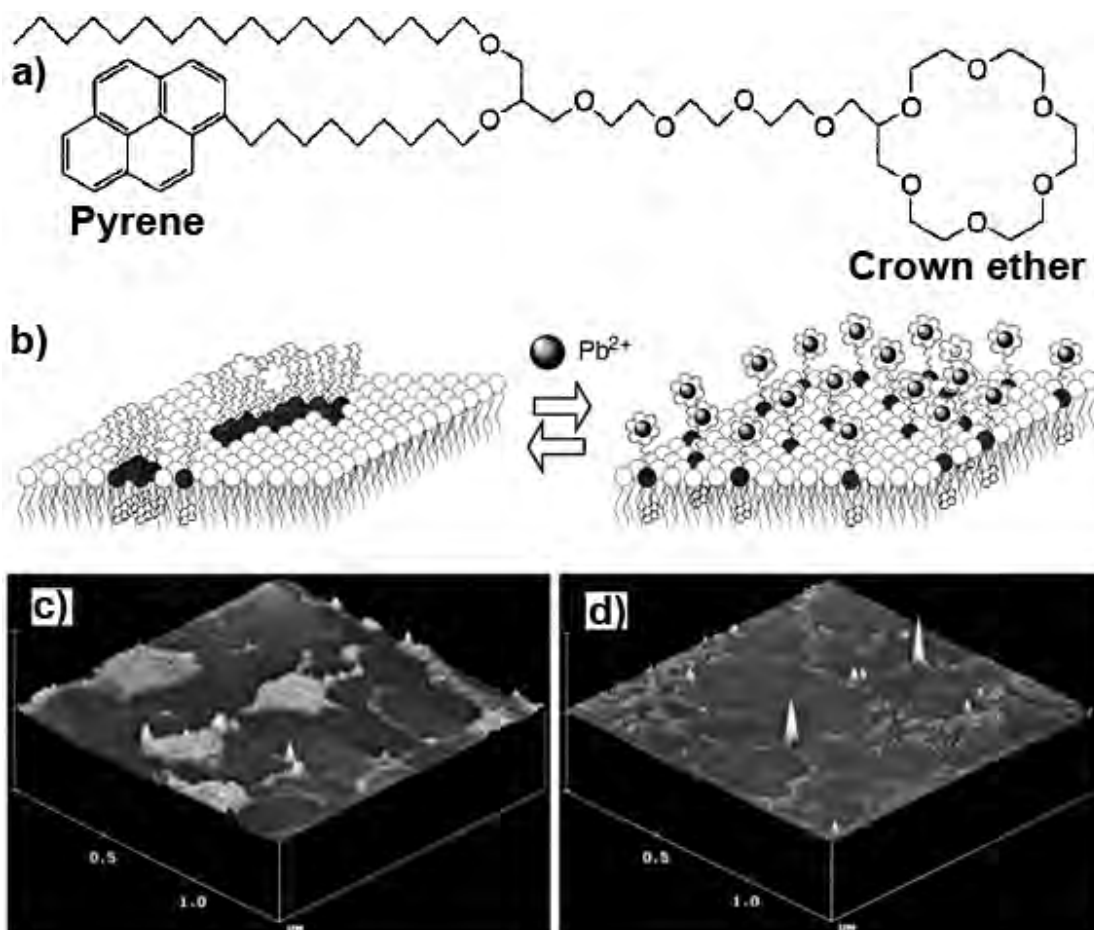


Figure 1.12 a) Crown six ether modified lipid with pyrene fluorophore, b) The response of crown ether modified lipid in phospholipid membrane with Pb^{2+} , c) an AFM image of bilayer before addition of Pb^{2+} , d) After addition of Pb^{2+} the aggregation was disappear.⁽³⁸⁾

Changing the receptor from crown ether to another cation receptor ligand gave similar results which the receptor lipid molecule changed from aggregation to dispersion by recognition the metal ion (Figure 1.13).⁽³⁹⁾ The bilayer response to select metal ions occurs as a change in ratio of the pyrene excimer to monomer fluorescence intensities (E/M). The excimer occurred by aggregation of pyrenes which shifted the emission of pyrenes to 470 nm whereas emission of pyrene monomer was 376 nm. Selectivity of metal ion recognition depended on the receptor groups; for example, 8-[1-Octadecyl-2-(9-(1-pyrenyl)nonyl)-rac-glyceroyl]-3,6-dioxaoctan-1-ol (PSOH), 8-[1-Octadecyl-2-(9-(1-pyrenyl)nonyl)-rac-glyceroyl]-3,6-dioxaoctan-1-ol (PSMA) and N-Methyl-2-[2-(2-[2-[3-octadecyloxy-2-(9-pyren-1-yl-nonyloxy)-propoxy]-ethoxy]-ethoxy)-ethoxy]-acetamide (PSIDA) have selectivity with Fe^{3+} higher than other metals salt while 6-[2-(2-[2-[3-Octadecyloxy-2-(9-pyren-1-yl-nonyloxy)-propoxy]-ethoxy]-ethoxy)-ethoxymethyl]-[2,29]bipyridine (PSBiPy) has higher selectivity toward Cu^{2+} .

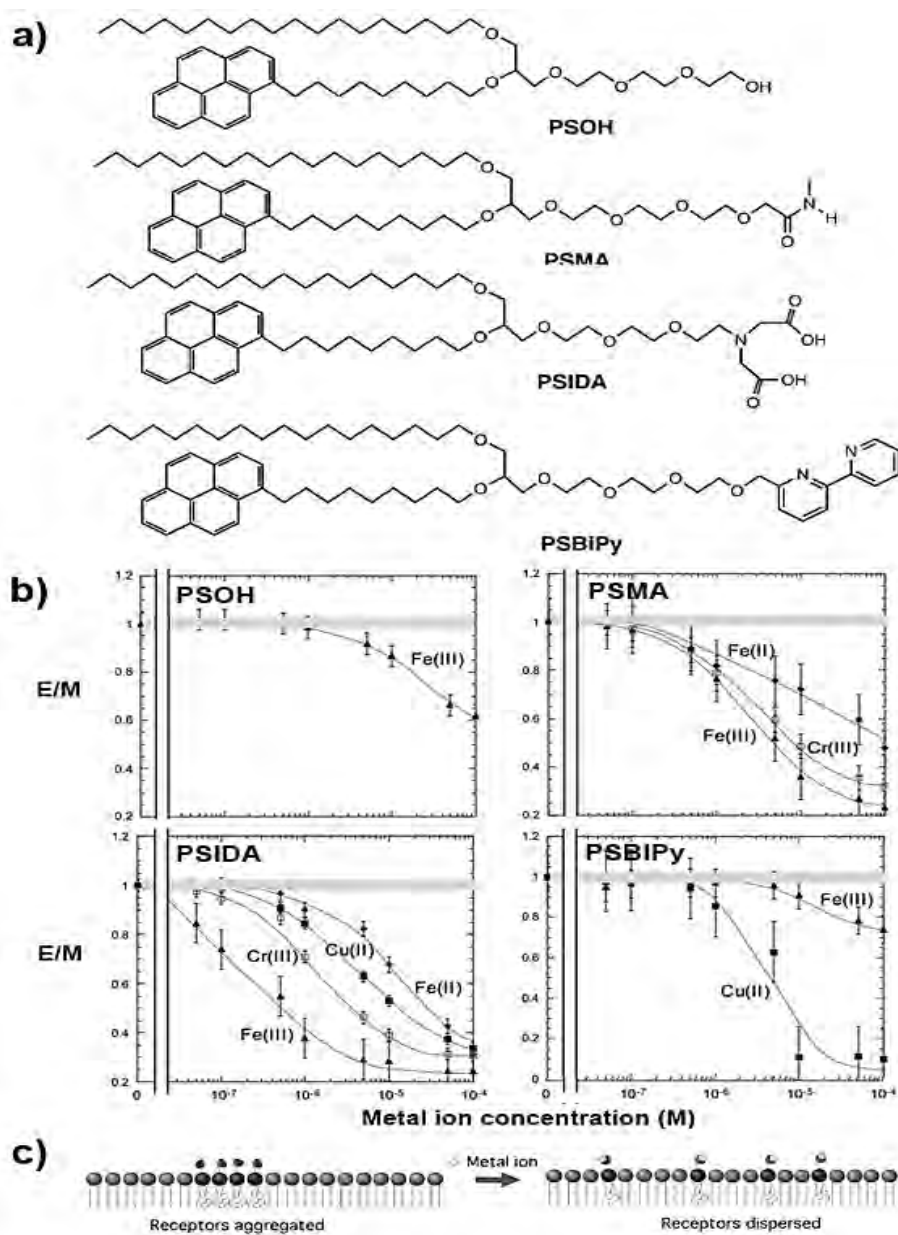


Figure 1.13 a) Molecular structure of pyrene-labeled receptor lipid, b) Fluorescence response (E=excimer, M= monomer,) vs metal ion concentration of 5% receptor/phospholipid bilayer, c) Illustration of the dispersion of initially aggregated receptor-lipids in a phospholipid membrane upon metal ion recognition.⁽³⁹⁾

In the metal ion membrane recognition, there has been possibility that lipid membrane can aggregate with metal ion especially divalent and trivalent metal ion. In the case of PSIDA/phospholipid vesicle, the columnar lipid bilayer stack was found after additional

Cu^{2+} . Coordination of Cu^{2+} complex with iminodiacetic acid produce the columnar lipid bilayer (Figure 1.14).⁽⁴⁰⁾

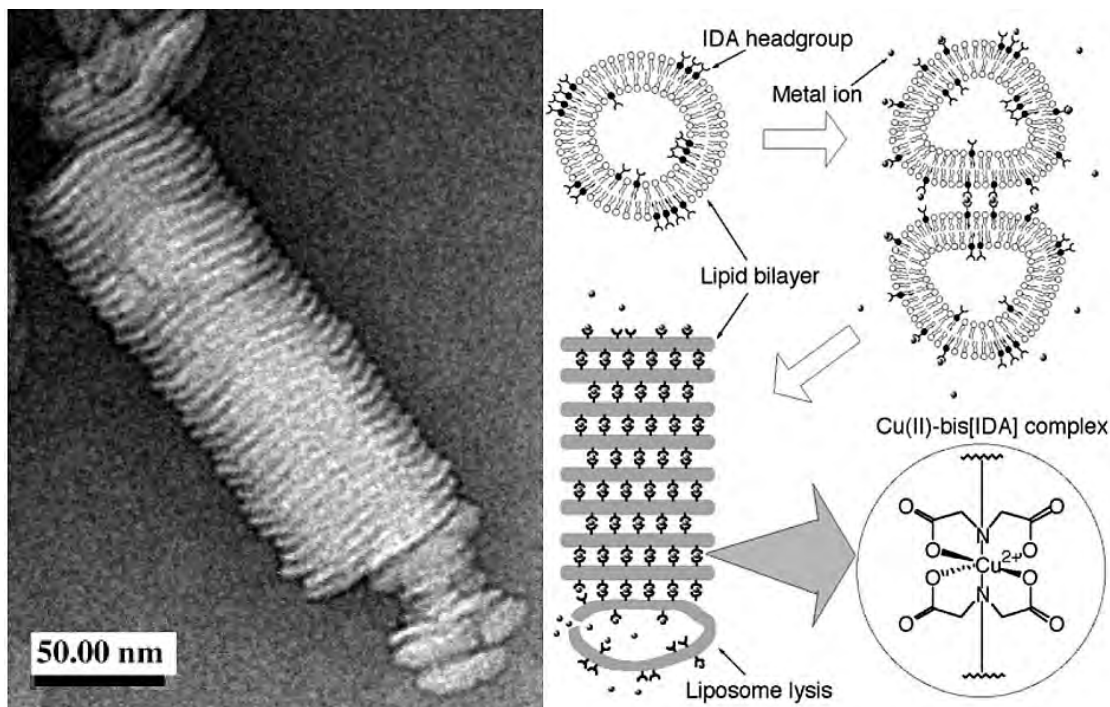


Figure 1.14 (left) TEM image of a self-assembled, columnar structured lipid bilayer stack that forms after Cu^{2+} addition to vesicle of 5%PSIDA/phospholipid, (right) proposed mechanism of lipid bilayer stack formation.⁽⁴⁰⁾

1.6 Oligo Ethylene glycol

Oligoethylene glycol is one of non-ionic surfactants. Solubility of oligoethylene glycol in aqueous solution is temperature dependence. Heating of oligoethylene glycol can interrupt hydrogen bonding between polymer and water molecule which lead to polymer aggregation. The temperature that polymer started to aggregate are called “Lower critical solution temperature (LCST)”. It is dependence on polymer chain length which is corresponding to the number of hydrogen bonding between polymer and water. For example, in 2002 Yin, X. and coworker reported the thermo-sensitive polymer by grafting methoxy poly(ethylene glycol) (MPEG) with different molecular weights into alternating copolymers of maleic anhydride, styrene monomer and 4-*tert*-butylstyrene (Figure 1.15a). They found that the cloud point temperature of polymer increase when molecular weight of oligoethylene glycol increase. This is because of intra/intermolecular hydrogen bonding and hydrophobic interaction of polymer (Figure 1.15b).⁽⁴¹⁾

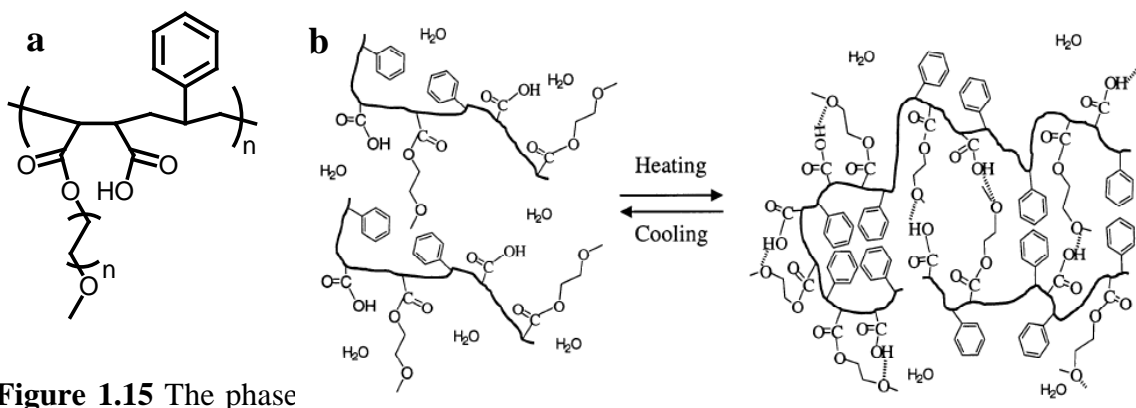


Figure 1.15 The phase transition of oligo ethylene glycol⁽⁴¹⁾

In 2005 Zhao, B. and coworker synthesized polystyrene grafting with methoxy ether of triethylene glycol, tetraethylene glycol and pentaethylene glycol (Figure 1.16). The grafting polystyrene has lower critical solution temperature in water.⁽⁴²⁾

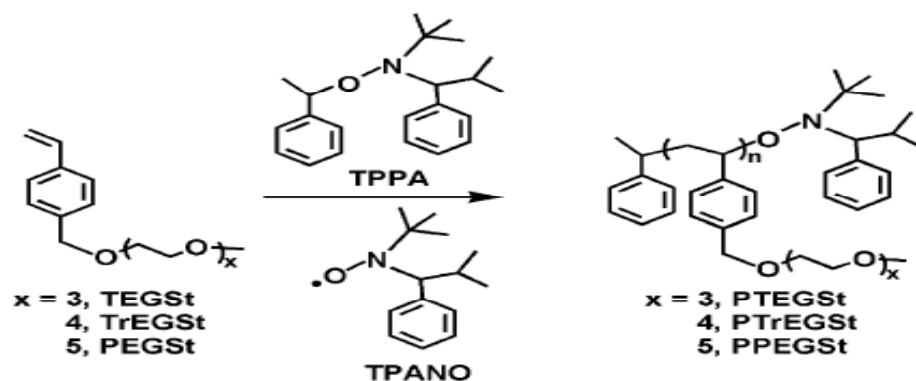


Figure 1.16 Synthesis of water soluble polystyrene ⁽⁴²⁾

In 2006 Li, D. and coworker synthesized polymer brush of poly (methoxydi(ethylene glycol) methacrylate) (PDEGMMA) and poly (methoxytri(ethylene glycol) methacrylate) (PTEGMMA) on silica nanoparticle. The nanoparticle showed thermo responsive properties which have cloud point at 25 and 48 °C respectively. ⁽⁴³⁾

In 2008 Saha, A. and coworkers reported about block-co-polymers having polyethylene glycol (PEG) segment with various numbers of ethylene glycol units (X= 4, 6, 8, 10) (Figure 1.17). The cloud point temperature of block-co-polymer is depended on hydrophobicity of the core and number of PEG unit. Increase hydrophobicity of the polymer resulted in decreasing the cloud point temperature. ⁽⁴⁴⁾

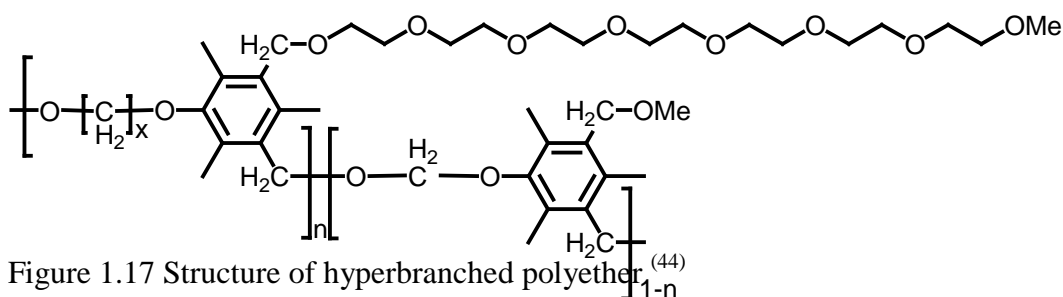


Figure 1.17 Structure of hyperbranched polyether ⁽⁴⁴⁾

Furthermore, there has been a report about interaction of ethylene glycol with metal ion. For example in 1995 French, R. and coworkers found diethylene glycol dimethyl ether and poly(ethylene oxide) can complex with lithium trifluoro methane sulfonate (LiCF_3SO_3). Raman and IR spectroscopy showed C-H bending of methylene group corresponding to the conformation change of ethylene glycol upon the formation of the complex. ⁽⁴⁵⁾

1.7 Lead ion (Pb^{2+})

The design of metal ion sensors had been a focus of research as it can detect toxic metal ion in real time application such as household industry and environment. One of the most toxic metal ions is lead ion (Pb^{2+}), it widely present in aquatic ecosystems. Monitoring of this highly hazardous metal ion on-site is an important issue for human health and environment. The very powerful and most currently used method for detection of Pb^{2+} is inductively coupled plasma mass spectrometry (ICPMS) but it requires expensive instruments and not suitable for on-site analyses. During the last decade, several Pb^{2+} sensing systems have been developed using various detection modes such as fluorometry,⁽⁴⁶⁻⁵⁵⁾ colorimetry⁽⁵⁶⁻⁶⁰⁾ and voltammetry⁽⁶¹⁻⁶⁵⁾.

In 2000 Deo, S. and co worker reported Pb^{2+} selective fluorescent probe. This probe consists of a fluorescent dye (dimethylamino)-naphthalene-1-sulfonamide (dansyl or dns) conjugated to the amino terminus of a tetrapeptide (ECEE; E = glutamate, C = cysteine). The dns-ECEE Pb^{2+} selective probe were monitored by fluorescence spectroscopy. Fluorescence spectra were obtained by exciting into the dansyl fluorophore absorption at 337 nm and scanning the emission from 400 to 800 nm. Upon addition of Pb^{2+} , the maximum emission of dns-ECEE shifts from 557 to 510 nm and increase in intensity (Figure 1.18). A plot of the ratio of the fluorescence emission intensity at 510 nm to the fluorescence emission intensity 557 nm (I_{510}/I_{557}) yields a calibration curve (Figure 1.18, inset) that gives an $\text{EC}_{50}^{\text{Pb}^{2+}}$ for the probe of $\sim 120 \mu\text{M}$.⁽⁶⁶⁾

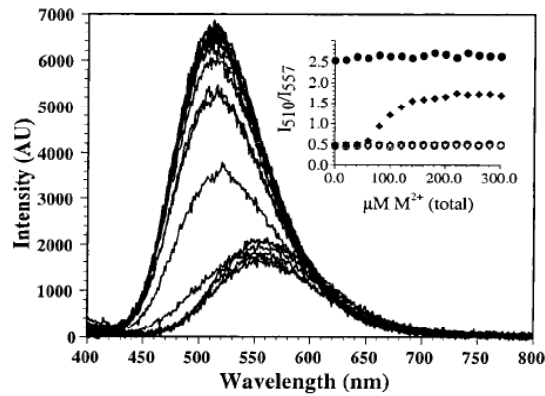


Figure 1.18 The fluorescence emission spectrum of the probe dns-ECEE shift upon addition of Pb^{2+} .⁽⁶⁶⁾

In 2003 Liu, J. and Lu, Y. reported the colorimetric Pb^{2+} sensor based on DNAzyme-directed assembly of gold nanoparticles. Functionalized gold nanoparticles with thiol-modified DNA to control distance between gold nanoparticles can be done by a linking DNA that is complementary to the DNA attached to nanoparticles. (Figure 1.19) When it approach each other and aggregate, the color of the gold nanoparticles changed from red to blue because of shifting in surface plasmon band to longer wavelength. Furthermore when in the presence of Pb^{2+} the 17E catalyzes hydrolytic cleavage of Sub_{Au} and prevents the formation of nanoparticle aggregates then red color appears as a result.⁽⁶⁰⁾

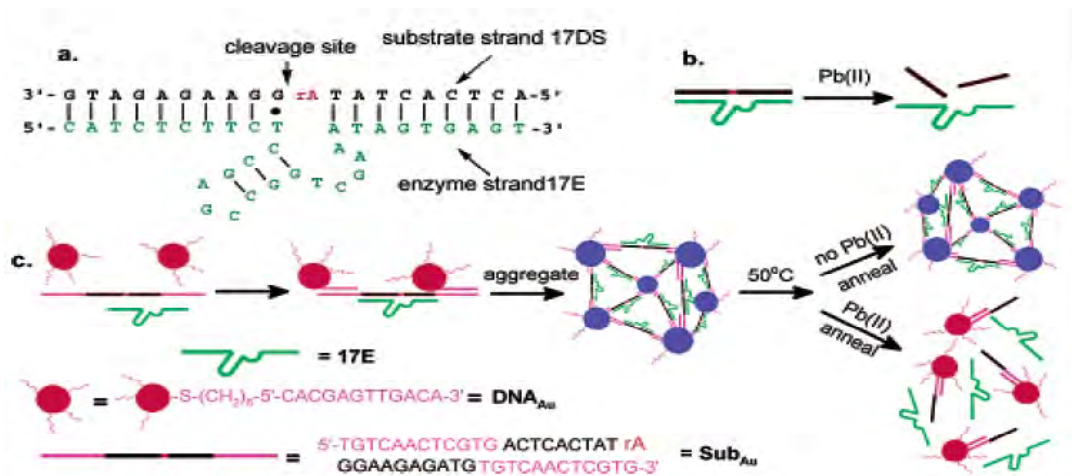


Figure 1.19 (a) Secondary structure of the “8-17” DNAzyme system that consists of an enzyme strand (17E) and a substrate strand (17DS). The cleavage site is indicated by a black arrow. Except for a ribonucleoside adenosine at the cleavage site (rA), all other

nucleosides are deoxyribonucleosides. (b) Cleavage of 17DS by 17E in the presence of Pb^{2+} . (c) Schematics of DNAzyme-directed assembly of gold nanoparticles and their application as biosensors for metal ions such as Pb^{2+} . In this system, the 17DS has been extended on both the 3' and 5' ends for 12 bases, which are complementary to the 12-mer DNA attached to the 13-nm gold nanoparticles (DNA_{Au}).⁽⁶⁰⁾

Several disadvantages from above literature such as required heat follow by a cooling process estimate 2 hour to observe color changes, which made practical onsite applications difficult then in 2004 Liu, J. and Lu, Y. reported an improved design that allows fast (<10 min) detection of Pb^{2+} at ambient temperature and improving the performance of the colorimetric sensor. This improvement of sensor performance is a result of detailed studies of the DNAzyme and nanoparticles, which identified “tail-to-tail” nanoparticle alignment and large (42 nm diameter) nanoparticle size as the major determining factors in allowing fast color changes. (Figure 1.20)⁽⁵⁹⁾

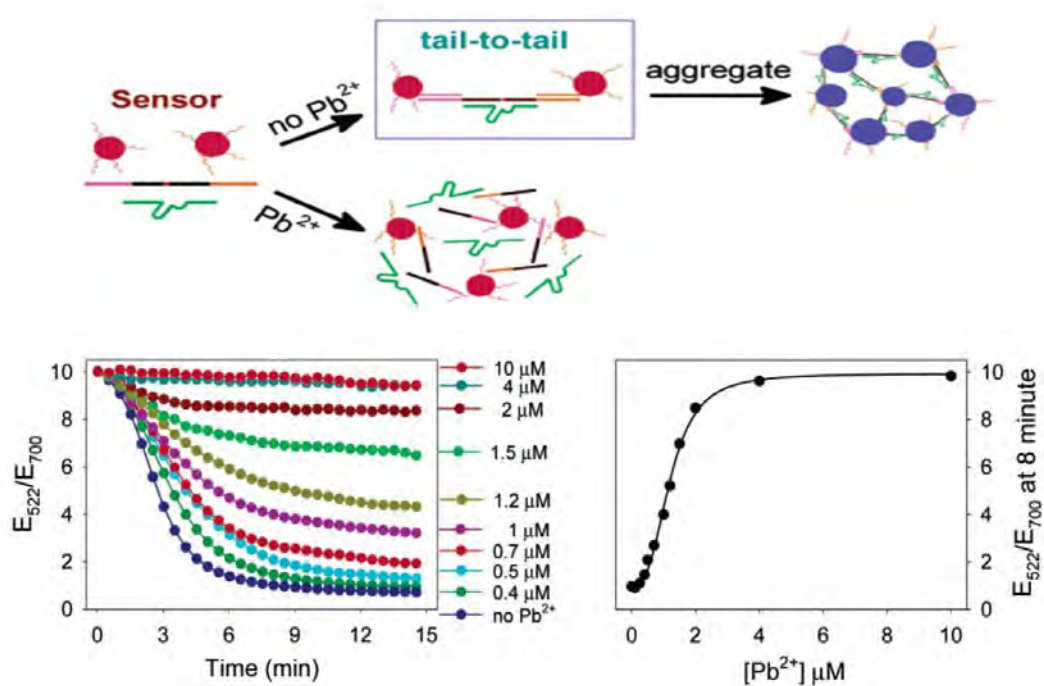


Figure 1.20 (a) Schematics of the new colorimetric sensor design. The nanoparticles are aligned in the “tail-to-tail” manner. In the absence of Pb^{2+} , nanoparticles can be assembled by the DNAzyme at ambient temperature within 10 min, resulting in a blue color; while in the presence of Pb^{2+} red color appeared because separation of

nanoparticles. **(b)** Kinetics of nanoparticle aggregation in the presence of different Pb^{2+} concentrations. **(c)** Extinction ratio at 8 min after the initiation of aggregation for different Pb^{2+} concentrations (from **b**).⁽⁵⁹⁾

In 2005 Kwon, J. Y. and co worker synthesized Pb^{2+} fluorescent probe from (2-aminoethyl)bis(2-pyridylmethyl)amine. Addition of Pb^{2+} to a colorless solution of probe in acetonitrile, pink color and the fluorescence characteristics of rhodamine B appear. The signal transduction occurs via reversible of CHEF (chelation-enhanced fluorescence). (Figure 1.21)⁽⁶⁷⁾

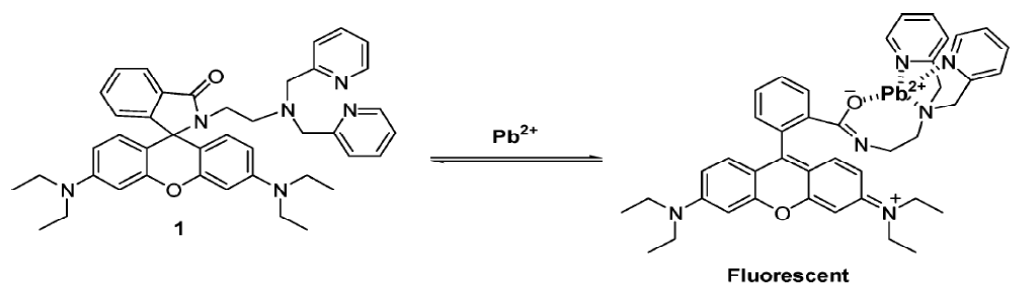


Figure 1.21 Mechanism for the fluorescent change of sensor after addition of Pb^{2+} .⁽⁶⁷⁾

In 2006; Xiao, Y. and coworker has been develop the electrochemical specific ion sensor for Pb^{2+} by immobilize “8-17” DNAzymes on electrode.⁽⁶⁸⁾ The sensor consists of a methylene-blue (MB) modified version of this catalytic DNA strand (**1**) hybridized to its complementary, 20-base substrate oligonucleotide (**2**). This complex is relatively rigid and presumably preventing the MB from approaching the electrode to transfer electrons (Figure 1.22, left). (Alternatively, transfer may occur through the double stranded DNA from a MB intercalated within the double-stranded regions of the sensing DNA). In the presence of Pb^{2+} , the trans-acting catalytic strand cleaves the sessile phosphodiester of the substrate into two fragments (Figure 1.22, middle). These fragments presumably dissociate from the complex, allowing the MB to transfer electrons to the electrode (Figure 1.22, right). In the absence of Pb^{2+} observe only small, reproducible Faradaic currents. A large increasing in Faradaic current was observed upon increasing Pb^{2+} . The directly measured detection limit of the current sensor architecture after 1 h incubation at $37\text{ }^\circ\text{C}$ is $0.3\text{ }\mu\text{M}$ (62 ppb), and the signal gain is linear over the range from 0.5 to $10\text{ }\mu\text{M}$ (104 to 2070 ppb).

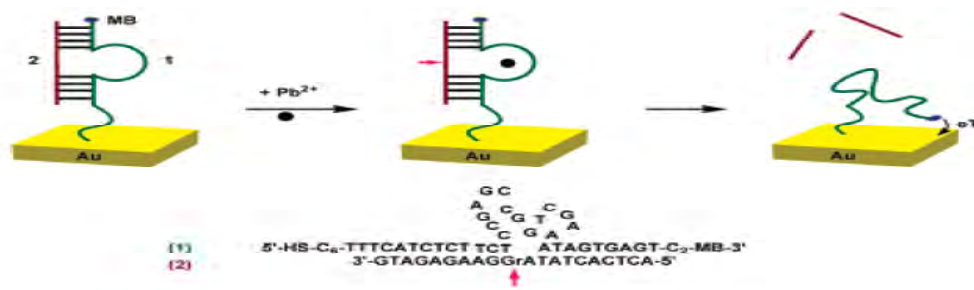


Figure 1.22 Schematic of the DNAzyme-Based Electrochemical Sensor. ⁽⁶⁸⁾

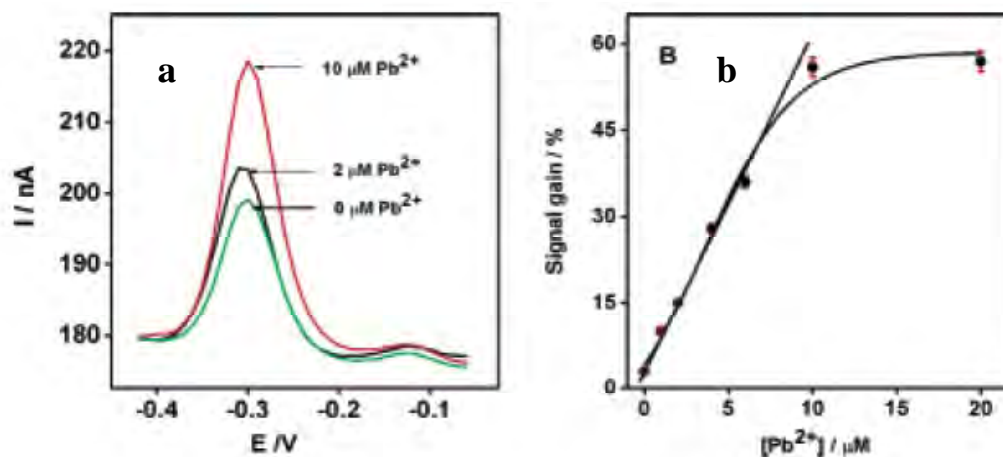


Figure 1.23 a) Shown are alternating current voltammograms of the sensor obtained after 1 h incubation at various Pb²⁺ concentrations. b) A dose-response curve for the lead sensor. ⁽⁶⁸⁾

In 2007 Zapata, F. and coworker has been reported a redox, chromogenic and fluorescent chemosensor molecule based on a deazapurine ring (2-ferrocenylimidazo[4,5-b]pyridine) selectively sensed aqueous Pb²⁺ in acetonitrile with detection limit of 1.32*10⁻⁸ M. ⁽⁴⁹⁾

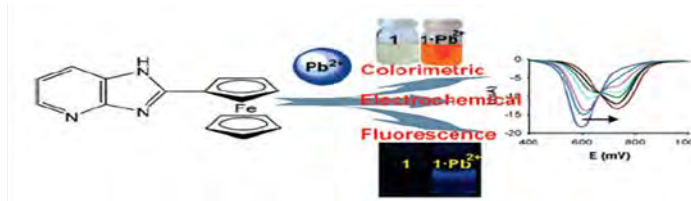


Figure 1.24 A redox, chromogenic and fluorescent chemosensor molecule. ⁽⁴⁹⁾

In 2007 Demeter, D. and coworker has been synthesized crown-annelaed oligothiophenes with a polyether loop attached at the two terminal thiophene rings and showed conformation transition in the presence of Pb^{2+} . UV-vis spectroscopy shows the changes induces in UV-vis spectrum. The addition of increasing amounts of Pb^{2+} produces a decrease in the intensity of the main absorption band in the 360-450 range and an increase of absorbance in the 250-340 nm. 1H NMR spectrometry shows the variation of the chemical shift of the various aliphatic protons versus the number of equiv of Pb^{2+} added. They suggest that the complexation of Pb^{2+} preferentially involves the two sulfur atoms attached to the thiophene rings. **(Figure 1.25).**⁽⁶⁹⁾

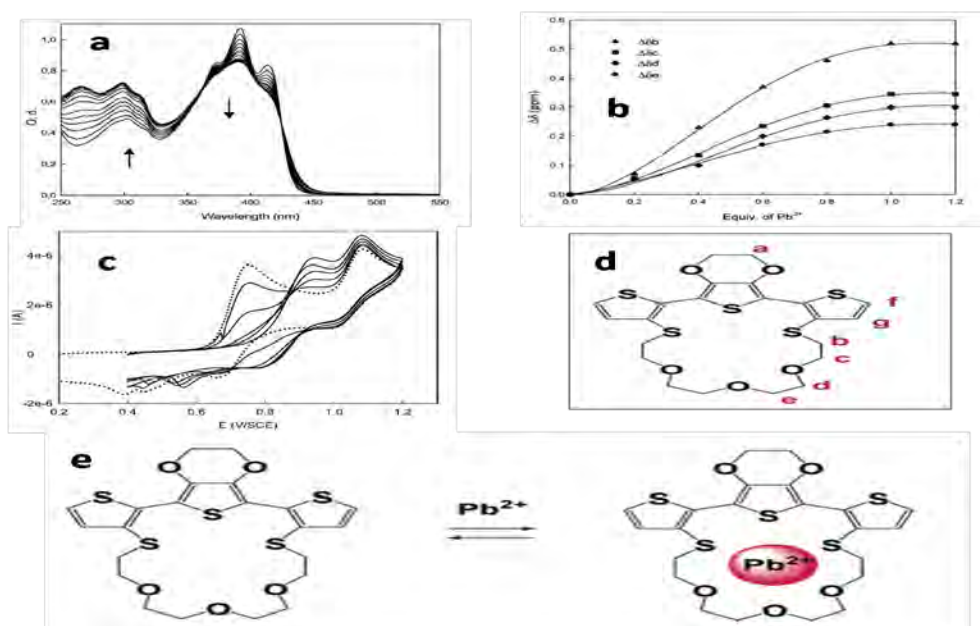


Figure 1.25 (a) UV-vis spectrum of crown-annulated terthiophenes (5×10^{-5} M in 1:1 CH_2Cl_2/CH_3CN) vs number of equiv of Pb^{2+} (b) Variation of chemical shifts of aliphatic protons (13.11 mM in 1:1 $CDCl_3/CD_3CN$) vs number of equiv of Pb^{2+} Initial spectrum 0 equiv and final spectrum 1.6 equiv by increments of 0.1 equiv. (c) CV of crown-annulated terthiophenes (0.5 mM in 0.1 0.1 M $Bu_4NPF_6/1:1$ $CHCl_3-CH_3CN$) in the presence of increasing amounts of Pb^{2+} . Dotted line corresponds to initial CV. (d) Aliphatic proton position of crown annulated terthiophenes (e) Schematic of crown-annulated terthiophenes complex with Pb^{2+} .⁽⁶⁹⁾

In 2010 Li, T. and coworker has been reported a colorimetric and chemiluminescence (CL) Pb^{2+} sensor based on a Pb^{2+} -induce allosteric G-quadruplex DNAzyme(PS2.M). In the presence of K^+ , PS2.M folds into a unimolecular G-quadruplex (with hemin as a cofactor) exhibit superior peroxidase-like activity and effectively catalyze the H_2O_2 -mediated oxidation of 2, 2'-azino-bis(3ethybenzothiazoline-6-sulfonic acid)diammonium salt (ABTS) or luminol to generate color change or CL emission. Addition of Pb^{2+} , induces K^+ -stabilized PS2.M to undergo a conformational transition, which is accompanied by a sharp decrease in the DNAzyme activity monitored in the ABTS- H_2O_2 or luminol- H_2O_2 reaction system (Figure 1.26). Two sensing systems provide different sensitivity for Pb^{2+} analysis. With colorimetry, Pb^{2+} can be detected at a level of 32 nM (~ 7 ppb), whereas the detection limit of Pb^{2+} is 1 nM (0.2 ppb) when utilizing the CL method.⁽⁵⁶⁾

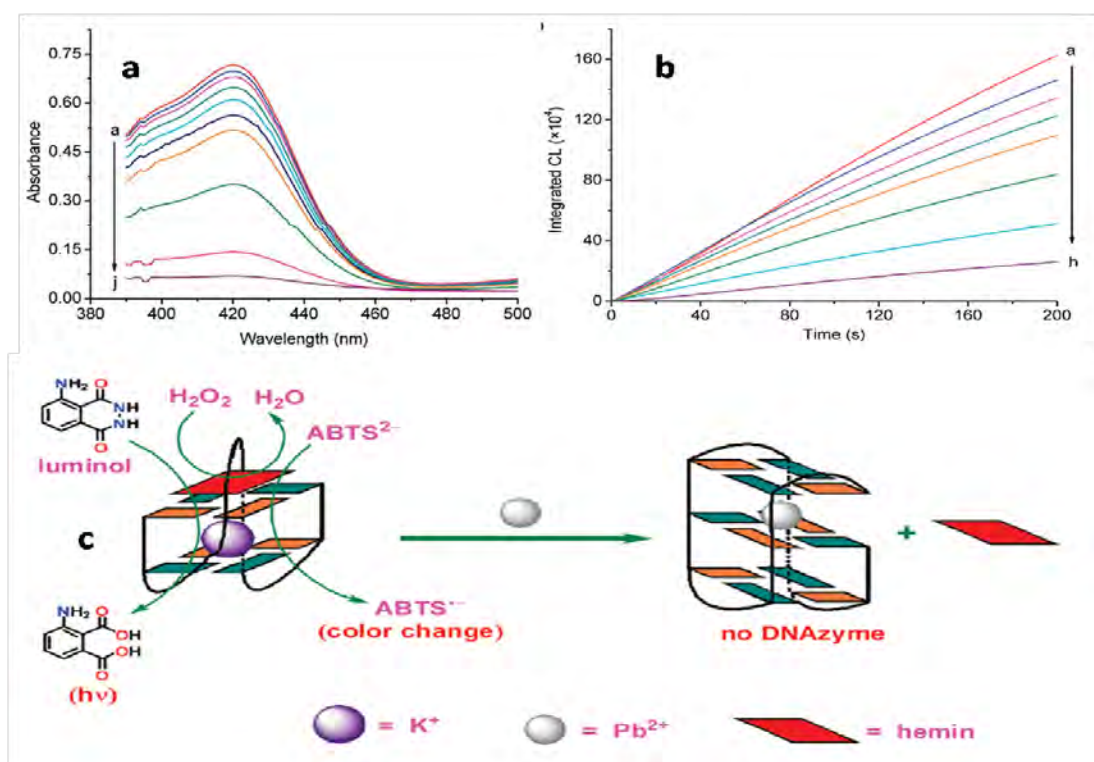


Figure 1.26 a) CL detection of Pb^{2+} using 10 nM PS2.M and 1 nM hemin in the luminol- H_2O_2 system: (a) CL integral curves for analyzing different concentrations of Pb^{2+} : 0 nM (curve a), 1 nM (curve b), 10 nM (curve c), 100 nM (curve d), 320 nM (curve e), 1 μ M (curve f), 2 μ M (curve g), and 10 μ M (curve h). **b)** Utilization of K^+ -stabilized PS2.M for

colorimetric Pb^{2+} analysis in the ABTS- H_2O_2 system: UV-vis absorption spectra (after 4 min) for utilizing 0.2 μM hemin-PS2.M to analyze different concentrations of Pb^{2+} : 0 nM (curve a), 32 nM (curve b), 100 nM (curve c), 320 nM (curve d), 1 μM (curve e), 3.2 μM (curve f), 10 μM (curve g), 20 μM (curve h), 40 μM (curve i), and 60 μM (curve j). **c**) Schematic of utilizing Pb^{2+} -induced allosteric G-quadruplex DNAzyme, PS2.M, for label-free colorimetric and CL detection of Pb^{2+} .⁽⁵⁶⁾

Sensors using organic synthetic ligands have low solubility in aqueous solution and cross-sensitivity toward other metal ions.^(49,69) While the uses of DNAzyme-based transducers showed much improved aqueous solubility, sensitivity and selectivity but there are high cost, low stability as well as lengthy and complicated sample preparation have so far prevented its practical applications.⁽⁵⁸⁻⁶⁰⁾ A low cost and stable transducer which can provide simple and selective detection of Pb^{2+} in aqueous media is thus highly desirable.

From above review oligo(ethylene glycol) had been installed as a pendant group in thermosensitive polymer to control water-solubility and thus cloud point of the polymers.⁽⁴¹⁻⁴³⁾ In this research, we would like to report the modification of PCDA with oligo(ethylene glycol) chains to be used incorporation with PCDA in constructing a sensitive selective colorimetric sensor for Pb^{2+} in aqueous media.

1.7 Objectives and scope of thesis

The objectives of thesis are

- 1) Synthesis and characterization of diacetylene monomers.
- 2) Study thermochromic properties and ion sensing ability of polydiacetylene
- 3) Improved sensitivity of polydiacetylene vesicles.
- 4) Development of Pb^{2+} sensors from polydiacetylene vesicle.

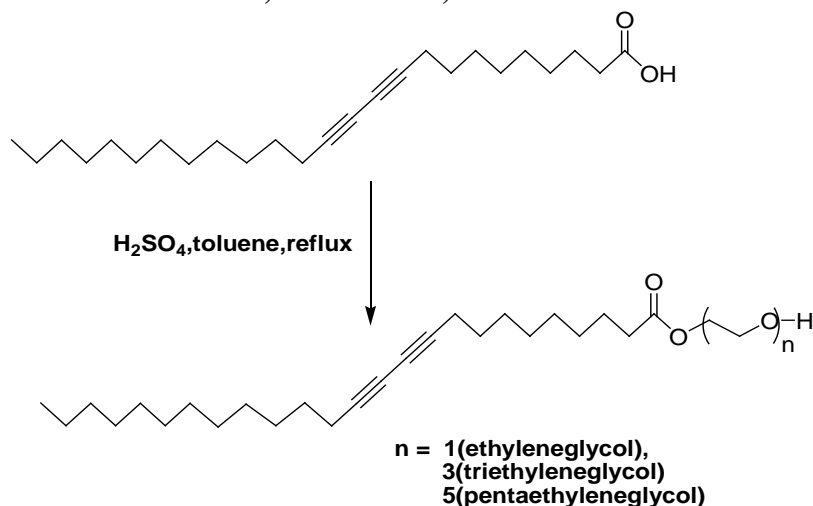
CHAPTER II EXPERIMENTAL

Materials: 10, 12-Pentacosanoic acid (PCDA) was purchased from GFS Chemical, USA. Other reagents were purchased from Sigma-Aldrich and Fluka. Analytical grade solvents such as chloroform and methylene chloride were used without further purification. Column chromatography was carried out on silica gel 60 (230-400 mesh; Merck). Thin layer chromatography (TLC) was carried out using Merck 60 F254 plates with a thickness of 0.25 mm. The diacetylene monomers were purified by filtration to remove the unintentionally polymerized lipid before use. For extraction and chromatography, the solvents were commercial grade and distilled before use except diethyl ether and chloroform which were reagent grade. Deionized water was used in all experiment involving aqueous media unless stated otherwise.

Analytical instruments: ^1H NMR and ^{13}C NMR spectra were recorded on a Varian Mercury 400 MHz NMR spectrometer (Varian, USA) using the residual solvent proton resonance of CDCl_3 at 7.26 ppm and 77 ppm as the reference. The electronic absorption spectra were recorded on a Varian Cary 100 Bio UV-Visible spectrophotometer (Varian, USA). Mass analysis was conducted with a Quattro micromass (Waters France) using the electrospray ionization (ESI). UV-irradiation was performed by UV light source (TUV 15W/G15 T18 lamp; Philips, Holland) at $900 \mu\text{w}/\text{cm}^2$. Sonication was performed by a Transonic T570/S ultrasonic bath (Elma, Germany).

2.1 Synthetic procedures

2.1.1 Synthesis of EG-PCDA, 3EG-PCDA, 5EG-PCDA



EG-PCDA: In a 50 mL round bottom flask with a magnetic stirring bar, (PCDA 332.1 mg 0.89 mmol) was dissolved in toluene (10 mL). Ethylene glycol (0.6 mL 10.77 mmol) and sulfuric acid (1 drop) were added. The mixture was then refluxed for 5 hours at 100 °C and the solvent was evaporated under reduced pressure. The residue were redissolved with CH_2Cl_2 (50 mL) and washed with saturated Na_2CO_3 solution (2×50 mL). The organic phase was collected and dried over anhydrous MgSO_4 and the solvent was removed in vacuo. The product was further purified by a column chromatography (hexane/ethyl acetate gradient from 0:100 to 20:80) yielding a white solid as the desired product (317.7 mg, 86% yield).

^1H NMR (400 MHz, CDCl_3): δ 4.22 (t, 2H, $\text{CH}_2\text{OC}=\text{O}$, $J = 4.6$ Hz), 3.83(m, 2H, CH_2O), 2.35 (t, 2H, $\text{CH}_2\text{C}=\text{O}$, $J = 7.5$ Hz) 2.24 (t, 4H, $\text{CH}_2\text{C}\equiv\text{C}-\text{C}\equiv\text{CCH}_2$, $J = 6.9$ Hz), 1.63 (m, 2H, CH_2), 1.51 (m, 4H, CH_2), 1.31 (m, 26H, CH_2), 0.88 (t, 3H, CH_3 , $J = 6.7$ Hz)

^{13}C -NMR (400 MHz, CDCl_3): δ 174.20 (C=O), 77.33 (C=C), 76.70(C=C), 65.94 (CH_2O), 65.31 (C=C), 65.21 (C=C), 61.39 (CH_2O), 34.16 (CH_2), 31.92 (CH_2), 29.65 (CH_2), 29.63 (CH_2), 29.61 (CH_2), 29.48 (CH_2), 29.35 (CH_2), 29.07(2C, CH_2), 29.05(CH_2), 28.88 (CH_2), 28.87 (CH_2), 28.74 (CH_2), 28.36 (CH_2), 28.29 (CH_2), 24.88 (CH_2), 22.68 (CH_2), 19.21 (CH_2), 19.19 (CH_2), 14.12 (CH_3)

3EG-PCDA : According to the above synthetic procedure and column chromatographic purification (hexane/ethyl acetate gradient from 0:100 to 40:60), 3EG-PCDA (348 mg, 73% yield) was obtained as a colorless viscous liquid from PCDA (348.4 mg, 0.93 mmol) and triethylene glycol (1.5 mL, 11.24 mmol).

^1H NMR (400 MHz, CDCl_3): δ 4.25 (t, 2H, $\text{CH}_2\text{OC}=\text{O}$, $J = 5.8$ Hz), 3.70(m, 10H, CH_2O), 2.35 (t, 2H, $\text{CH}_2\text{C}=\text{O}$, $J = 7.6$ Hz) 2.25 (t, 4H, $\text{CH}_2\text{C}\equiv\text{C}$, $J = 7.0$ Hz), 1.63 (m, 2H, CH_2), 1.52 (m, 4H, CH_2), 1.32 (m, 26H, CH_2), 0.89 (t, 3H, CH_3 , $J = 6.8$ Hz)

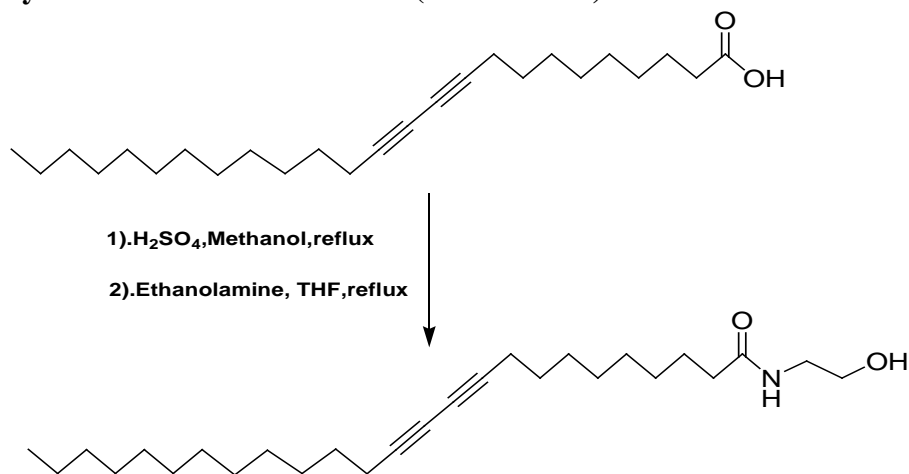
^{13}C -NMR (400 MHz, CDCl_3): δ 173.82 ($\text{C}=\text{O}$), 77.32 ($\text{C}\equiv\text{C}$), 76.68($\text{C}\equiv\text{C}$), 72.47 (CH_2O), 70.58 (CH_2O), 70.38 (CH_2O), 69.23 (CH_2O), 65.30 ($\text{C}\equiv\text{C}$), 65.22 ($\text{C}\equiv\text{C}$), 63.21 (CH_2O), 61.78 (CH_2O), 34.15 (CH_2), 31.91 (CH_2), 29.64 (CH_2), 29.62 (CH_2), 29.60 (CH_2), 29.47 (CH_2), 29.34 (CH_2), 29.09(2C, CH_2), 29.05(CH_2), 28.90 (CH_2), 28.86 (CH_2), 28.76 (CH_2), 28.35 (CH_2), 28.31 (CH_2), 24.85 (CH_2), 22.68 (CH_2), 19.21 (CH_2), 19.19 (CH_2), 14.10 (CH_3)

5EG-PCDA: According to the above synthetic procedure and column chromatographic purification (hexane/ethyl acetate gradient from 0:100 to 60:40), 5EG-PCDA (309.3 mg, 62% yield) was obtained as a colorless viscous liquid from PCDA (312.8 mg, 0.85 mmol) and pentaethylene glycol (2 mL, 9.46 mmol).

^1H NMR (400 MHz, CDCl_3): δ 4.22 (t, 2H, $\text{CH}_2\text{OC}=\text{O}$, $J = 4.8$ Hz), 3.67(m, 18H, CH_2O), 2.32 (t, 2H, $\text{CH}_2\text{C}=\text{O}$, $J = 7.6$ Hz) 2.23 (t, 4H, $\text{CH}_2\text{C}\equiv\text{C}$, $J = 7.0$ Hz), 1.61 (m, 2H, CH_2), 1.50 (m, 4H, CH_2), 1.30 (m, 26H, CH_2), 0.87 (t, 3H, CH_3 , $J = 6.8$ Hz)

^{13}C -NMR (400 MHz, CDCl_3): δ 173.80 ($\text{C}=\text{O}$), 77.32 ($\text{C}\equiv\text{C}$), 76.68($\text{C}\equiv\text{C}$), 72.55 (CH_2O), 70.63 (CH_2O), 70.60 (CH_2O), 70.58(CH_2O), 70.33(CH_2O), 70.11(CH_2O), 69.23 (CH_2O), 65.30 ($\text{C}\equiv\text{C}$), 65.21 ($\text{C}\equiv\text{C}$), 63.21 (CH_2O), 61.73 (CH_2O), 34.16 (CH_2), 31.90 (CH_2), 29.63 (CH_2), 29.61 (CH_2), 29.59 (CH_2), 29.46 (CH_2), 29.33 (CH_2), 29.08(2C, CH_2), 29.06(CH_2), 28.90 (CH_2), 28.85 (CH_2), 28.76 (CH_2), 28.35 (CH_2), 28.31 (CH_2), 24.85 (CH_2), 22.67 (CH_2), 19.20 (CH_2), 19.18(CH_2), 14.10 (CH_3)

2.1.2. Synthesis of amido derivative (NEG-PCDA).



In a 50 mL round bottom flask equipped with a magnetic stirrer, a solution of PCDA (302.6 mg, 0.81 mmol) in methanol (25 mL) was added with a catalytic amount of sulfuric acid (one drop) and refluxed for 3 hours at 65 °C. The resulting mixture was evaporated under reduced pressure, redissolved with CH₂Cl₂ (50 ml) and washed with Na₂CO₃ (2 x 50 mL). The organic phase was collected, dried over anhydrous MgSO₄ and the solvent was removed in vacuo. The residue was dissolved in THF (25 mL) and ethanolamine (0.5 mL, 8.2 mmol) was added at room temperature. After refluxing overnight, the solvent was removed under reduced pressure and the residue was purified by silica gel column chromatography (40/60Hexane/ethyl acetate) yielding a white solid as the desired product (232.8 mg, 69% yield,)

¹H-NMR (400 MHz, CDCl₃): δ 5.88 (s, 1H, NH), 3.74 (m, 2H, CH₂N), 3.45(m, 2H, CH₂O), 2.23 (m, 6H, CH₂C≡C, CH₂C=O), 1.64 (m, 2H, CH₂), 1.52 (m, 4H, CH₂), 1.32 (m, 26H, CH₂), 0.89 (t, 3H, CH₃, *J* = 6.8 Hz)

¹³C-NMR (400 MHz, CDCl₃): δ 173.80 (C=O), 77.32 (C≡C), 76.68(C≡C), 65.29 (C≡C), 65.20 (C≡C), 62.54 (CH₂O), 42.45 (CH₂N), 36.61 (CH₂), 31.89 (CH₂), 29.62 (CH₂), 29.60 (CH₂), 29.58 (CH₂), 29.45 (CH₂), 29.32 (CH₂), 29.15 (CH₂), 29.11(CH₂), 29.07(CH₂), 28.87 (CH₂), 28.84 (CH₂), 28.72 (CH₂), 28.34 (CH₂), 28.26 (CH₂), 25.63 (CH₂), 22.66 (CH₂), 19.18 (CH₂), 19.16(CH₂), 14.09(CH₃)

2.2 Preparation of polydiacetylene (PDA) sols

The diacetylene monomer, 10,12-pentacosadiynoic acid (PCDA), was dissolved in diethyl ether and filtered to remove the unintentionally polymerized material. The filtrate was dried under a rotary evaporator to give a white solid. A stock solution of PCDA was prepared by dissolving a controlled amount of PCDA in chloroform and kept in refrigerator for further use.

For preparation of poly(PCDA) sol, a known amount of PCDA was pipetted from the stock solution into a round-bottomed flask followed by rotary evaporation to remove the solvent. A known volume of Milli-Q water was added and the suspension was heated to 75-85 °C, followed by sonication in an ultrasonic bath for 30 min when a semitransparent or transparent sol was obtained. The sol was kept in a refrigerator overnight before irradiated with UV light (256 nm, 15 watt) for 1 min and filtered through a filter paper (Watchhman No.1) to give clear intense blue-color poly(PCDA) sol.

Preparation of mixed lipid PDAs sols were accomplished by the following method. A known amount of PCDA was pipetted from the stock solution into a test tube and mixed with the known amount of another diacetylene monomer (selected from EG-PCDA, 3EG-PCDA 5EG-PCDA and NG-PCDA) in dichloromethane at various mixing ratio. The solvent was removed by flowing nitrogen gas over the solution to dryness. After the organic solvent was removed, MiliQ water was added to yield the final concentration of the mixed monomers of 0.1 mM. The lipid suspension was sonicated at 75-80 °C for 30 minutes to obtain a clear sol. After sonication, the sol was kept in a refrigerator for 24 h and the polymerization was carried out by UV irradiation (256 nm, 900 watt/cm²) for 1 minute at room temperature.

2.3 Study of thermochromism

The absorbance at 540 nm of the mixed lipid (0.1 mM) PDA was monitored from 20-80 °C by a temperature controlled UV-vis spectrophotometer (Varian Cary 100 Bio, Varian, USA) using a heating rate of 1 °C/minute. The absorbance values were plotted against the temperature.

2.4 Study of colorimetric responses of the PDA sols to metal ions

The colorimetric response of the PDA sols to metal ions were studied by addition of a metal ion stock solution (i.e. LiCl, NaCl, KCl, CaCl₂, MgSO₄, CdCl₂, Co(OAc)₂, Cu(OAc)₂, FeCl₂, HgCl₂, Ni(OAc)₂, Pb(NO₃)₂, and Zn(OAc)₂; 10 mM) into each PDA sol. The final concentrations of metal ion and the PDA were 100 μM and 0.1 mM, respectively. The mixtures were allowed to stand at room temperature for 30 minute prior to observation data recording. The color appearance of the mixtures was photographically recorded and their electronic absorption spectra were collected by UV-Vis spectrophotometer. The quantitative evaluation of the colorimetric response (%CR) was determined as the percentage of the change of the blue color fraction (FB₀-FB) against the initial blue color fraction (FB₀) according to the following equation: %CR = 100 × (FB₀-FB)/FB₀. FB is the blue fraction calculated from $A_{\text{blue}}/(A_{\text{blue}}+A_{\text{red}})$ where A_{blue} and A_{red} are the absorbance at the λ_{max} of the blue and the red forms of the PDAs, respectively. For Pb²⁺ and Zn²⁺ ions, the colorimetric responses at various metal ion concentration(5-100 μM) were also determined.

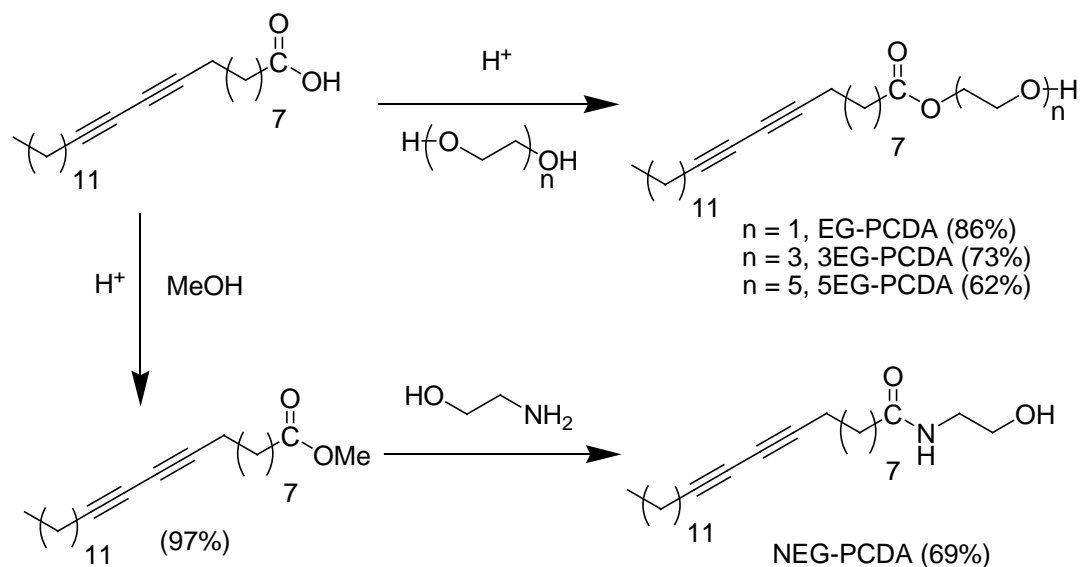
CHAPTER III

RESULTS AND DISCUSSION

Oligo(ethylene glycol) chains have been reported that they can be used for increasing water solubility and thermal responsive properties of polymers. They have also been widely used for preventing aggregation in many nanoparticulate systems.⁽⁴¹⁾ Furthermore, they can also form ion channels in lipid membranes and increase fluidity of the membrane by reducing membrane crystallinity. In this thesis, four derivatives of 10, 12-pentacosadiynoic acid containing ethylene glycol (EG), triethylene glycol (3EG) and pentaethylene glycol (5EG), and ethanolamine (NEG) were synthesized as their corresponding esters (EG-PCDA, 3EG-PCDA, 5EG-PCDA) and amide NEG-PCDA. Polydiacetylene (PDA) sols containing ethylene glycol modified PCDA were prepared and studied for their metal ion sensing applications. The thermal colorimetric responses of the sols led to some understanding of the role of the ethylene glycol chains.

3.1 Synthesis of glycol-modified PCDA derivatives

Three ethylene glycol esters and an ethanolamido derivatives of PCDA were synthesized and studied as modulators for poly(PCDA) sensors. Ethylene glycol (EG-PCDA), triethylene glycol (3EG-PCDA) and pentaethylene glycol esters (5EG-PCDA) were synthesized by simple acid catalyzed esterification of PCDA with ethylene glycol and the corresponding oligo(ethylene glycol).⁽⁷⁰⁾ The preparation of the amido derivative, NEG-PCDA, was performed via a condensation between the methyl ester of PCDA and ethanolamine.⁽⁷¹⁻⁷³⁾ The desired products were all obtained in good yields after silica gel column chromatographic purification (**Scheme 3.1**).



Scheme 3.1 Synthesis of three ethylene glycol esters and one ethanolamido derivatives of PCDA

The ethylene glycols ester derivatives of PCDA were synthesized by simple acid catalyzed esterification of PCDA with ethylene glycol, triethylene glycol and pentaethylene glycol respectively. The oligo(ethylene glycol) ester derivatives 3EG-PCDA and 5EG-PCDA were liquids at room temperature except EG-PCDA was solid state. The desired product was isolated by column chromatography with 86%, 73% and 62% yield.

The ethylene glycols esters derivatives of PCDA were characterized by $^1\text{H-NMR}$ spectroscopy. A triplet signal corresponding to the methylene group (**u**) adjacent to the oxygen atom of the ester group appeared around δ 4.22-4.25 ppm (**Figure 3.1**). The integral ratio of signal of the methylene protons at hydroxy group (**v**) and methylene protons in oligo(ethylene glycol) groups were 1:1, 1:5 and 1:8 respectively implied to increased in chain length of oligo(ethylene glycol) The integral ratio of the signal of the methylene protons adjacent to the carbonyl group, methylene protons adjacent to the hydroxyl group and those next to the esterate

oxygen was 1:1 indicating the monosubstituted product connected with three oligo(ethylene glycol). Mass spectrum of EG-PCDA, 3EG-PCDA and 5EG-PCDA also showed the molecular ion peak at 418.6, 528.7[M+Na]⁺ and 617.9[M+Na]⁺ respectively

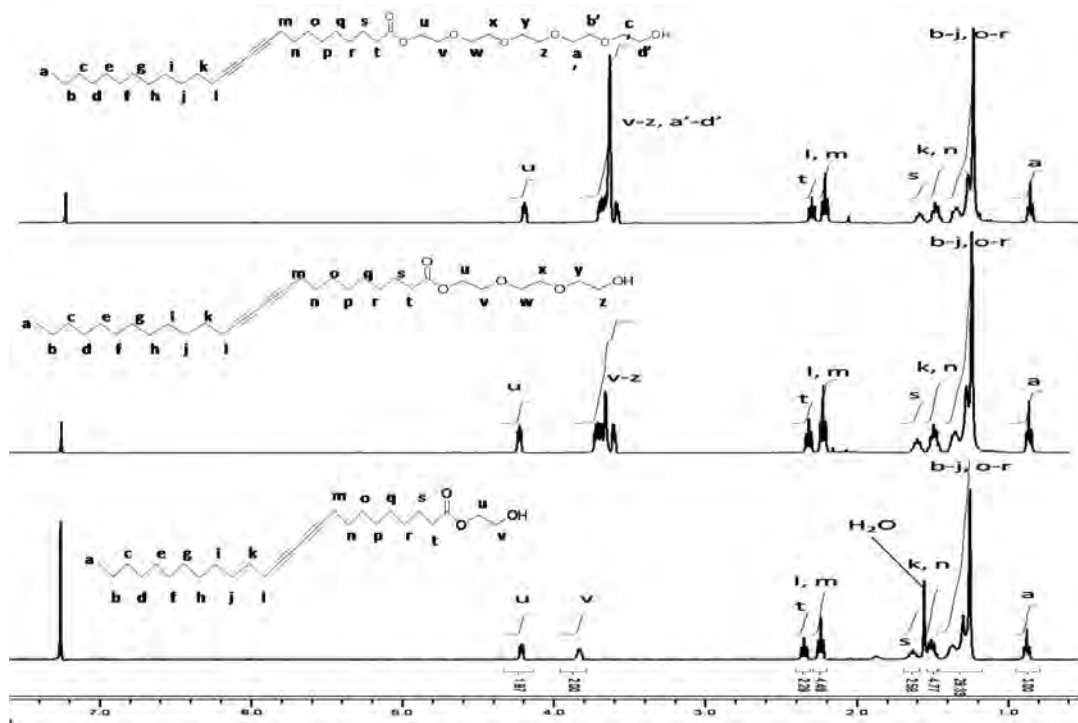


Figure 3.1 ¹H-NMR spectrum of EG-PCDA, 3EG-PCDA and 5EG-PCDA in CDCl₃

The synthesis of NEG-PCDA was performed via a condensation between the methyl ester of PCDA and ethanolamine. (**Scheme 3.1**). The desired product was isolated by column chromatography as white solid with 69% yield. The NEG-PCDA was characterized by ¹H-NMR spectroscopy. A singlet signal at δ 5.88 ppm (**u**) is corresponding to the proton adjacent to nitrogen atom. A triplet signal corresponding to the methylene group adjacent to the nitrogen atom of the amide group appeared at δ 3.75 ppm (**v**) indicated to substitution of ethanolamine in PCDA molecule (**Figure 3.2**). Mass spectrum also showed the molecular ion peak at 417.6 m/z.

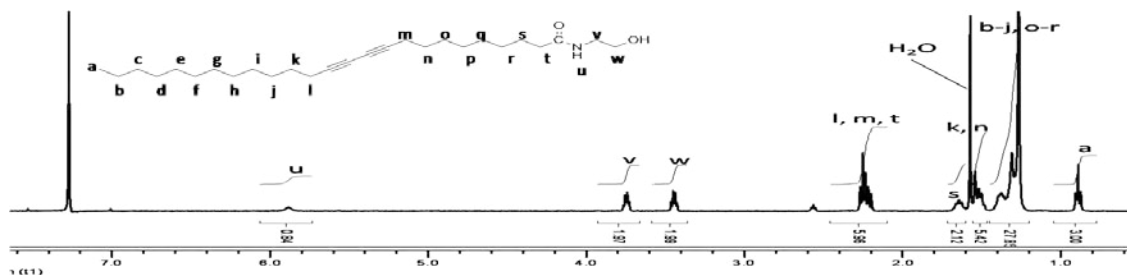


Figure 3.2 $^1\text{H-NMR}$ spectrum of NEG-PCDA in CDCl_3 .

3.2 Preparation of diacetylene sols and their polymerization

The oligo(ethylene glycol) ester derivatives i.e. 3EG-PCDA and 5EG-PCDA were liquids at room temperature which can be frozen and photopolymerized to form deep blue PDAs by UV irradiation. These lipids dispersed well in milli-Q water by ultrasonication (340 W) for 30 min at 75 °C but the resulting sols remained colorless after UV irradiation at 0-5 °C. The results suggested that molecular self assemblies of these lipids in aqueous media did not meet the topological requirement for diacetylene polymerization.⁽¹⁻⁴⁾ that is in contrast to the parent PCDA which can be polymerized into a blue polydiacetylene in both solid and aqueous sol states. However, the EG-PCDA and NEG-PCDA sols prepared under similar condition were polymerizable to form a red and blue PDA, respectively. It is interesting to note that the carboxylic acid and amide but not the ester group can provide the necessary hydrogen bonding. The hydrogen bonding among the head groups of the diacetylene lipids has been found to be essential for the formation of blue PDA from this class of diacetylene monomers.⁽¹⁵⁾

To investigate the effect of oligo(ethylene glycol) chains on the molecular assembly of PCDA and its sensing properties, mixed lipid PDA sols of EG-PCDA/PCDA, 3EG-PCDA/PCDA, 5EG-PCDA/PCDA and NEG-PCDA/PCDA were prepared at various mixing ratios. The mixed diacetylene lipid aqueous suspensions were sonicated at 75-85 °C. After sonication, the mixed diacetylene lipids appeared as translucent hydrocolloids which were stored at 4 °C overnight before being irradiated with UV light (254 nm, 900 $\mu\text{W}/\text{cm}^2$) for 1 min at room temperature to give blue sols of the corresponding PDAs (**Figure 3.3a**). The blue PDA sols were obtained from the mixed lipids containing up to 50% mole of the esters while the mixed lipids containing 80% mol of the esters remained colorless indicating no polymerization. The blue color of polymerized mixed lipid containing 50% mole of 3EG-PCDA and 5-EG-PCDA is however considerably paler

than those from the mixed lipid containing 30% mole of the PCDA esters. The blue sol showed an electronic absorption band in the visible range with λ_{max} at 590 and 640 nm (**Figure 3.3b**) corresponding the π - π^* transition with the double bond vibronic coupling characteristic for the ene-yne conjugated backbone of PDAs.

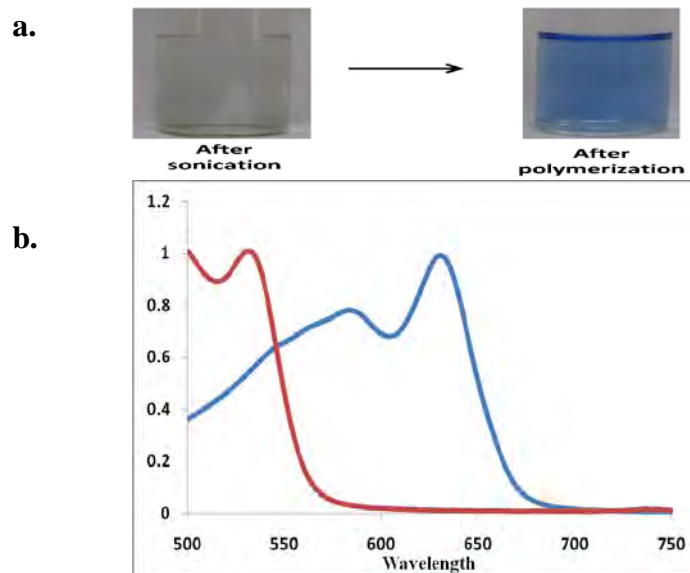


Figure 3.3 (a) Color photographs mixed diacetylene lipid (total concentration is 0.1mM) in Milli-Q water left after sonication at 75 °C right after UV irradiation for 1 min. (b) electronic absorption band of mixed lipid PDA containing 30% PCDA ester

3.3 Thermochromism of mixed lipid PDA sols

Apparently, the incorporation of EG-PCDA, 3EG-PCDA, 5EG-PCDA and NEG-PCDA to PCDA caused the color transition from blue to red shifted to lower temperatures (Figure 3.4-3.7). However, more detail effects of the types and contents of the modified PCDA on the color transition temperature could not be drawn from this simple appearance observation.

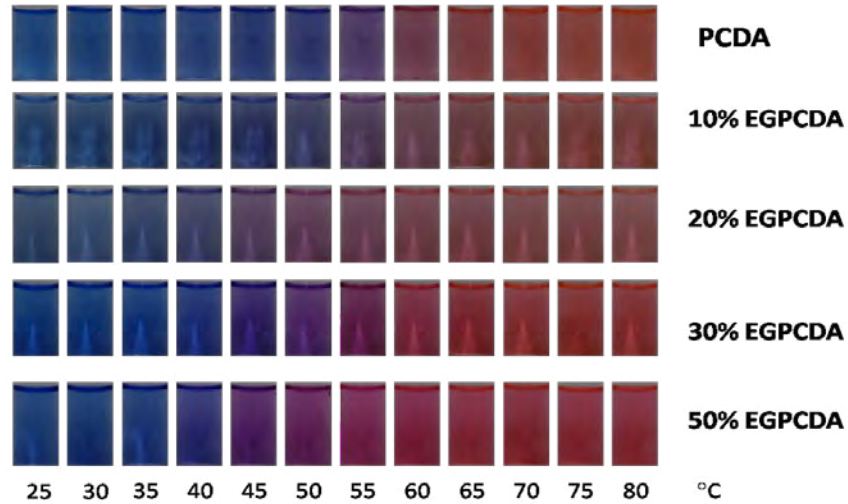


Figure 3.4 Thermochromism photographs of EG-PCDA/PCDA

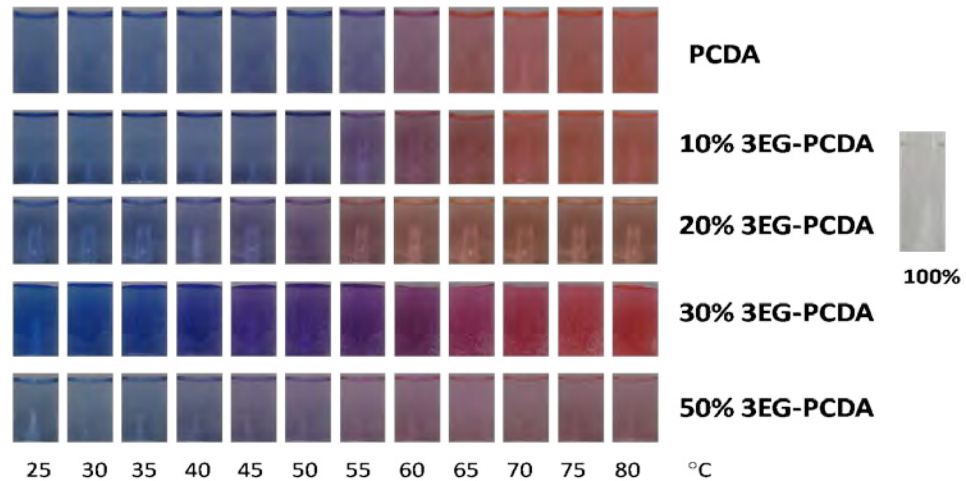


Figure 3.5 Thermochromism photographs of 3EG-PCDA/PCDA

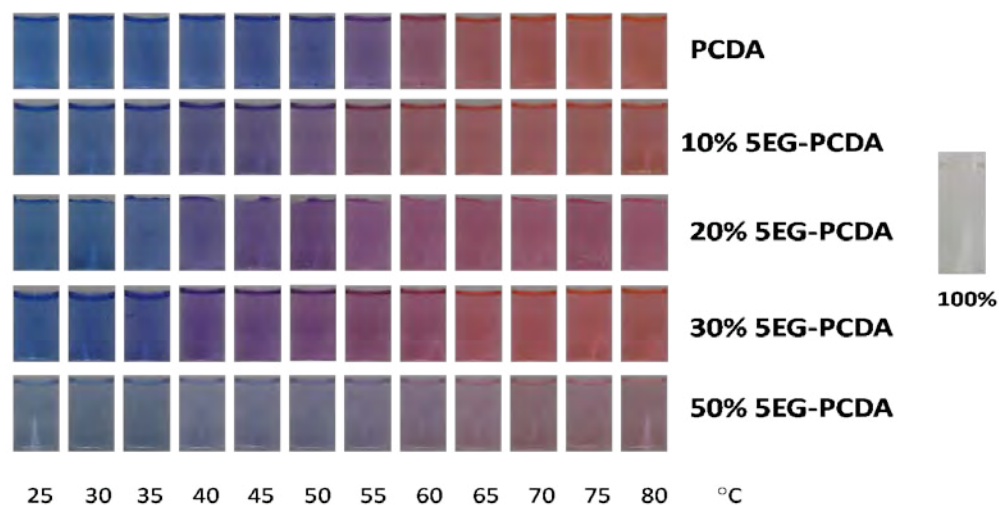
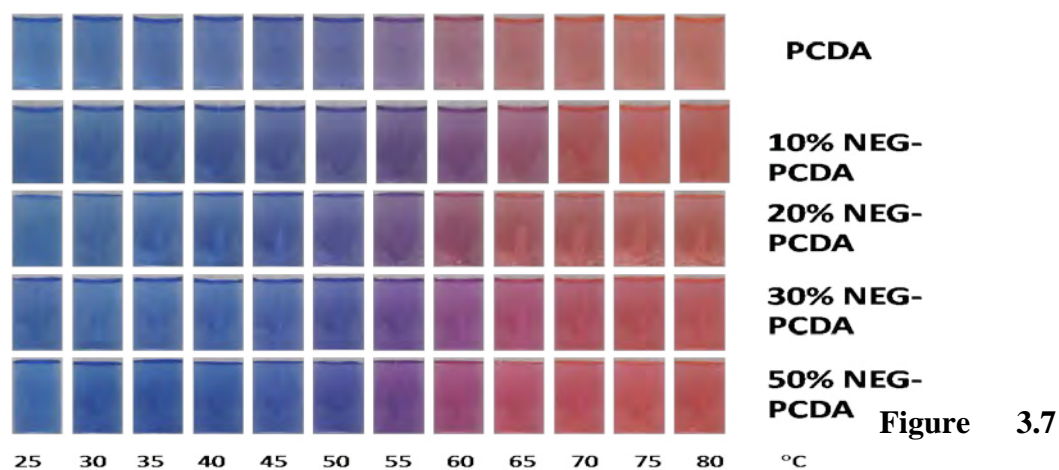


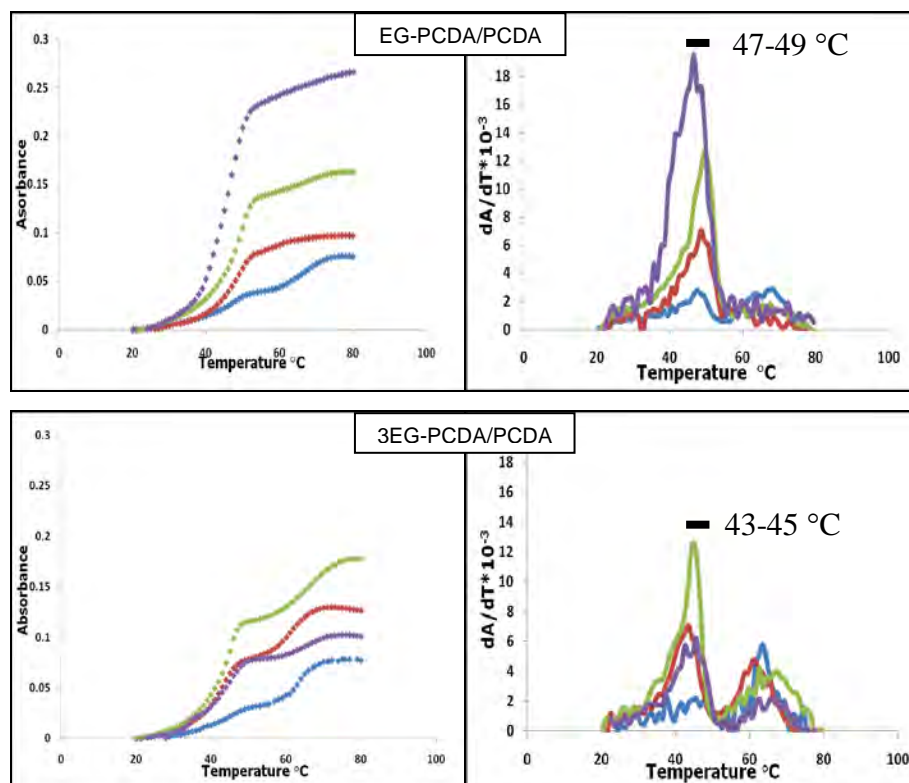
Figure 3.6 Thermochromism photographs of 5EG-PCDA/PCDA



Thermochromism photographs of NEG-PCDA/PCDA

To study the effects of the types and contents of the glycol modified PCDA lipids, the color transitions of these mixed lipid sols were thus monitored by temperature variable UV-vis spectrophotometer from 20 to 80 °C. The plot of the absorbance of the red phase PDA at 540 nm against the temperature showed that the absorbance (A) of the sols increased with the temperature (T) in correspondence to the blue to red color change. **Figure 3.8** show the first derivative ($\Delta A/\Delta T$) plot revealed more insightful features of the color transition process of the mixed lipid sols. of the EG-PCDA, 3EG-PCDA and 5EG-PCDA showed two steps of color transition while the NEG-PCDA mixed lipid sols exhibited continuous one-stepped color transition. In the two-stepped color transition, the second step observed around 65 °C is the same as the color transition temperature of

poly(PCDA)⁽²⁴⁾ while the first step appeared at 48, 44 and 41°C for EG-PCDA/PCDA, 3EG-PCDA/PCDA and 5EG-PCDAPCDA respectively. Furthermore the decreasing of first transition step related to the increase of the oligo(ethylene glycol) chain length(**Figure 3.9**). The absorbance change in the first transition step also clearly increased with the content of the PCDA ester up to at least 30% mole in the mixed lipid.



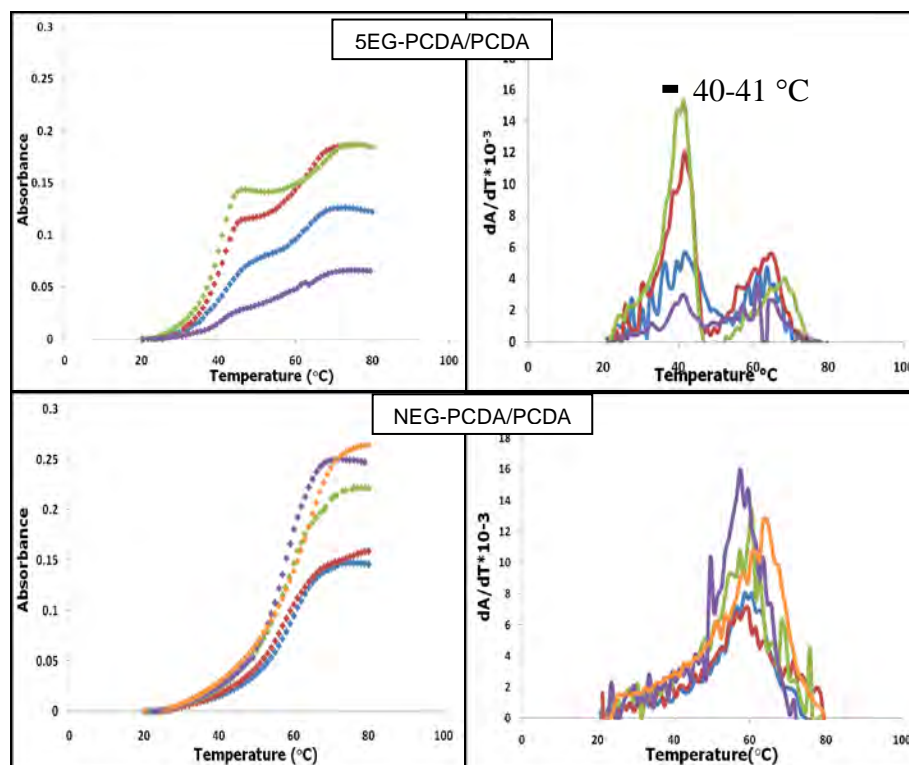


Figure 3.8 Temperature dependence of the absorbance (A) at 540 nm of the mixed lipid sols (left) and their first derivative, dA/dT (right). The absorbance of each sol was set to zero at 20 °C. The black bars indicate transition temperature ranges obtained from the maxima in the derivative plots; 10% ■; 20% ■; 30% ■; 50% ■; 100% ■.

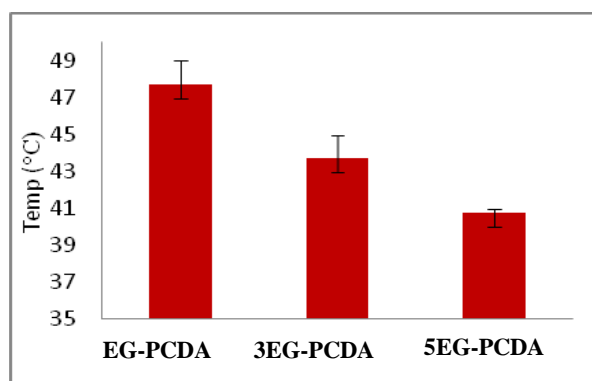


Figure 3.9 First transition temperature of EG-PCDA/PCDA, 3EG-PCDA/PCDA and 5EG-PCDA/PCDA

Since pure PCDA ester does not form blue PDA vesicles, the first color transition step is likely to be derived from a copolymer between the PCDA ester and PCDA within the mixed lipid vesicles. The amount of the copolymer increases with the PCDA ester with an expense of PCDA homopolymer. From the results of EG-PCDA/PCDA, the absorbance change of the first step mixed lipid sols increased up to 50% mol of EG-PCDA where the second color transition corresponding to poly(PCDA) was totally disappeared. However, for 3EG-PCDA/PCDA and 5-EG-PCDA/PCDA sols, the absorbance change of the first transition step increased only up to 30% mol the PCDA esters. The results may be attributed to the poor vesicle formation of the mixed lipid at higher content of 3EG-PCDA and 5EG-PCDA as evidenced by the pale color of the sols prepared at 50% mole content of these PCDA esters. The difference between the highest content of the PCDA esters being incorporated into the mixed lipid sols implies that the copolymer formed between PCDA and its esters are of different ratios.

The observation of one-stepped color transition of NEG-PCDA/PCDA sol suggested that only one type of PDA is formed, most likely a copolymer between NEG-PCDA and PCDA. The NEG-PCDA/PCDA sols also exhibited transition temperature lower than the sols of pure NEG-PCDA ($\sim 63\text{ }^{\circ}\text{C}$) and pure PCDA ($\sim 65\text{ }^{\circ}\text{C}$)⁽²⁴⁾, and decreased with the increase of NEG-PCDA content in the range of 10-50% mole. The hydrogen bond forming secondary amide group in NEG-PCDA is probably a main contributor to this thermochromic behavior which is very different from those of the mixed lipid sols containing PCDA esters. From the above discussion, the mixed lipid polydiacetylene PCDA-ester/PCDA ester showed two transition temperatures suggesting two distinct structures of polydiacetylenes. It is reasonable to assume that the PDAs were obtained from diacetylene lipids assembled in a blockwise fashion rather than a random or alternated assembly (Figure 3.10). The random or alternated PDAs should exhibit only one transition temperature liked the one observed for NEG-PCDA/PCDA. Referring to the non-polymerizability of pure 3EG-PCDA and 5EG-PCDA sols, it is not likely that the block of pure PCDA-ester can be polymerized. Hence, the block structure of the polymers should consist of alternated PCDA-ester/PCDA and separate PCDA block. This proposed structure fit well with the two-stepped thermochromism having two transition temperatures, one below and one equal to that of poly(PCDA).

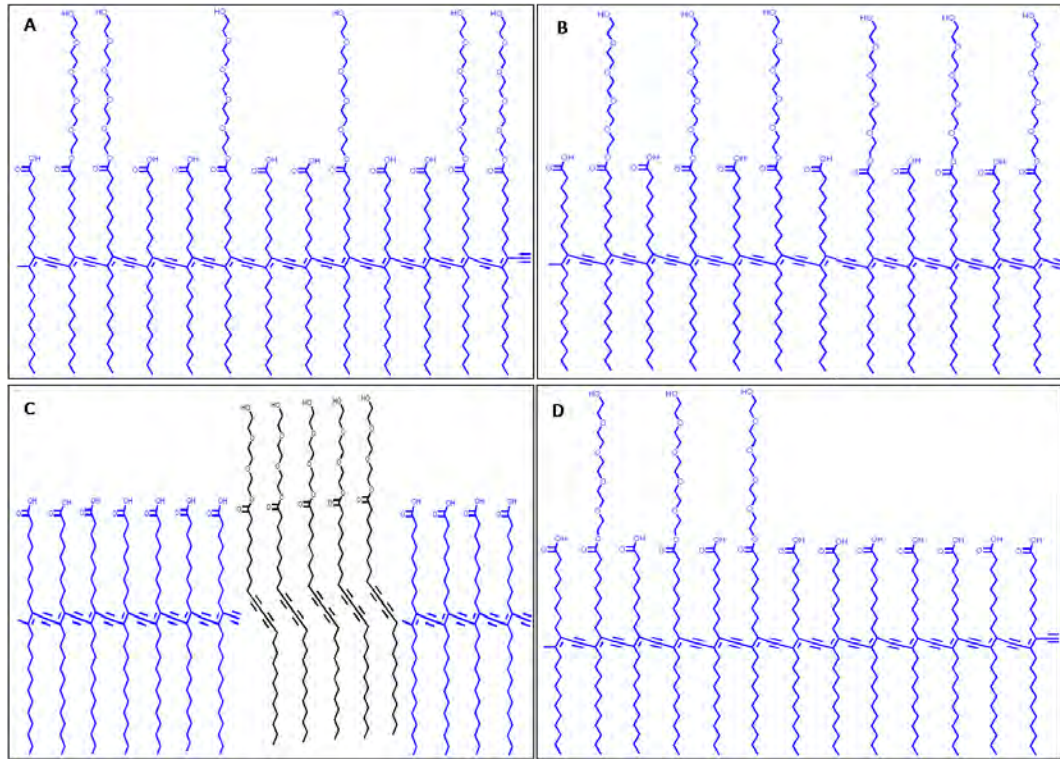


Figure 3.10 Possible structures of PDA derived from the mixed lipids of EG-PCDA, 3EG-PCDA and 5EG-PCDA/PCDA: a) random, b) alternate, c) block and d) alternated block

3.4 Development of metal ion sensor from polydiacetylene mixed vesicles

Contamination of natural water and soil by heavy metal ions has been one of most serious environmental problems. To control and prevent the contaminants spreading through ecological food chain, promptly and thoroughly field tests are necessary. An appropriate detecting system should be simple to use and inexpensive as the extensive on-site test can involve a vast field area and myriad numbers of samples. The color change of polydiacetylene mixed vesicles is easy to be observed by naked eyes that may be developed into an instrument less detecting system.

3.4.1 Colorimetric sensing to metal ions

To apply the mixed lipid sols for colorimetric detection of heavy metal ions, an aqueous solution of metal salts such as CdCl_2 , Co(OAc)_2 , Cu(OAc)_2 , FeCl_2 , HgCl_2 , Ni(OAc)_2 , $\text{Pb(NO}_3)_2$, and Zn(OAc)_2 was added to the mixed lipid sols containing 30% mole of PCDA esters. At 100 μM , only Pb^{2+} caused a distinct color change of the sol from blue to red for only 5EG-PCDA/PCDA sol (**Figure 3.11**). The colorimetric response (%CR) of the sols to the metal ions recorded at 30 minutes after mixing showed the highest %CR of 55% for 5EG-PCDA/PCDA sol in the presence of Pb^{2+} (**Figure 3.11**). Significantly lower %CRs of 20% and 10% were observed for 3EG-PCDA/PCDA and EG-PCDA/PCDA sols, respectively. To our delight, 5EG-PCDA/PCDA sol also showed excellent selectivity toward Pb^{2+} with Zn^{2+} gave significantly lower %CR of 15%.

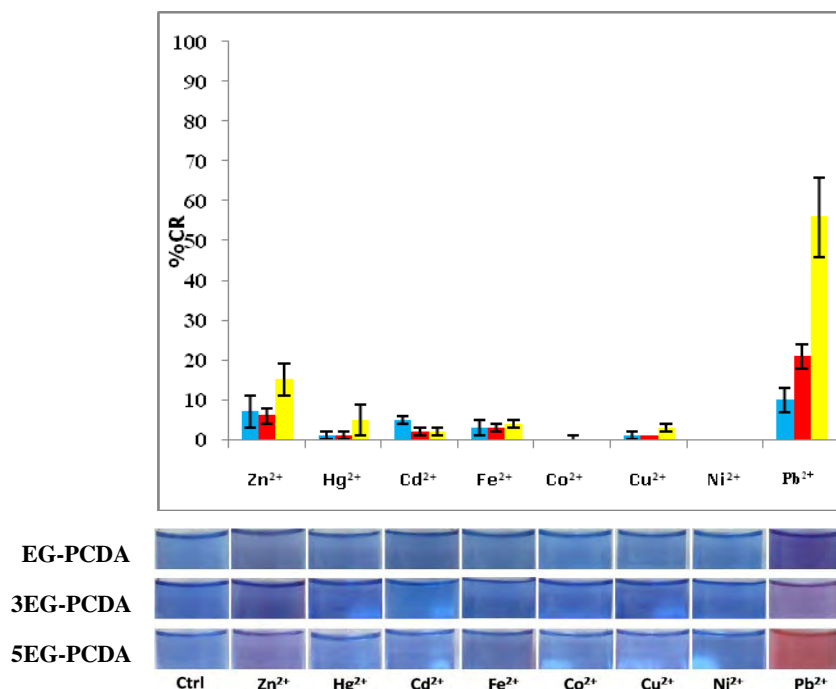


Figure 3.11 Colorimetric responses (%CR) of the mixed lipid PDA sols containing 30% mole of EG-PCDA (■), 3EG-PCDA (■) and 5EG-PCDA (■) upon addition of metal ions (100 μ M). The photograph underneath the histogram is the visual appearance of the corresponding sols.

Oligo(ethylene glycol) chains and crown ethers are well known ionophores for alkali ions and has been known to form ion channel in lipid membrane.⁽⁴¹⁾ There is also a literature report proposed that the crown ether is responsible for lead ion recognition in lipid membrane.⁽³⁸⁾ According to the thermochromic sensitivity results of the mixed lipid sols, we however suspected that the oligo(ethylene glycol) chains act as a sensitivity enhancer while the carboxylic/carboxylate groups of PCDA are responsible for the Pb²⁺ selectivity. To substantiate this proposition two pure lipid and three mixed lipid PDA sols *viz.* PCDA, NEG-PCDA, 5EG-PCDA/NEG-PCDA (30/70% mol), 5EG-PCDA/PCDA (30/70% mol) and 5EG-PCDA/PCDA/NEG-PCDA (30/35/35% mol) were prepared and studied. There is no colorimetric response (%CR ~ 0) observed upon the addition of 100 μ M of Pb²⁺ to the sols having no carboxylic head group (**Figure 3.12**) denoted that the carboxylic/carboxylate groups are responsible for the ion binding because. As for the sols containing carboxylic head group, the %CR increased with the incorporation of 30%

mole of 5EG-PCDA probably attributed to the membrane fluidity enhancement by lowering the collaborative hydrogen bonding on the vesicle surface. These results agree well with the thermochromic behavior of the mixed lipid sols described earlier. It is also interesting to note that replacing half of PCDA (35% mole) with NEG-PCDA resulted in lower colorimetric response in correspondence to the lower numbers of carboxylic/carboxylate groups available for Pb^{2+} binding.

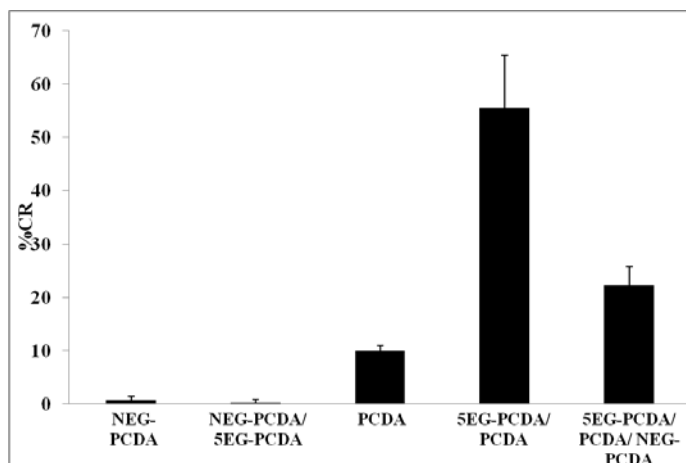


Figure 3.12 Colorimetric responses (%CR) to Pb^{2+} (100 μM) of PDA sols prepared from NEG-PCDA, 5EG-PCDA/NEG-PCDA (30/70% mol), PCDA, 5EG-PCDA/PCDA (30/70% mol), and 5EG-PCDA/PCDA/NEG-PCDA (30/35/35% mol).

The Pb^{2+} induced color change of the PDA sols was also investigated by dynamic light scattering (DLS) technique and atomic force microscopy (AFM). Although 5EG-PCDA/PCDA vesicles were relatively fragile, several round shaped objects with diameters of ~ 100 nm remained observable in the AFM image of a dry sample of 5EG-PCDA/PCDA sol on mica surface and DLS technique (**Figure 3.13a, c**). The average particle of PDA containing 100 μM Pb^{2+} showed increased in particle sizes of PDA from 100 nm (red line) to 160 nm and 1700 nm (green line) and image of the dry sol containing 100 μM Pb^{2+} clearly showed large aggregation and fusion of the PDA vesicles (**Figure 3.13b**) suggesting that the color transition involved multiple coordination between the vesicle spheres and Pb^{2+} ions (**Figure 3.13d**).

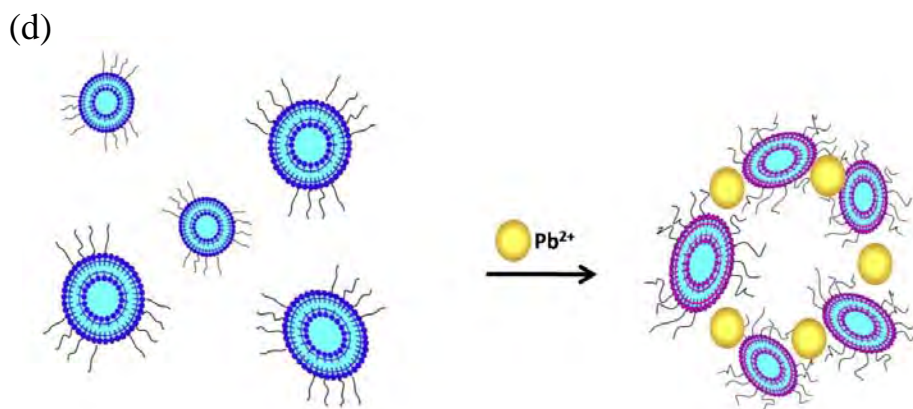
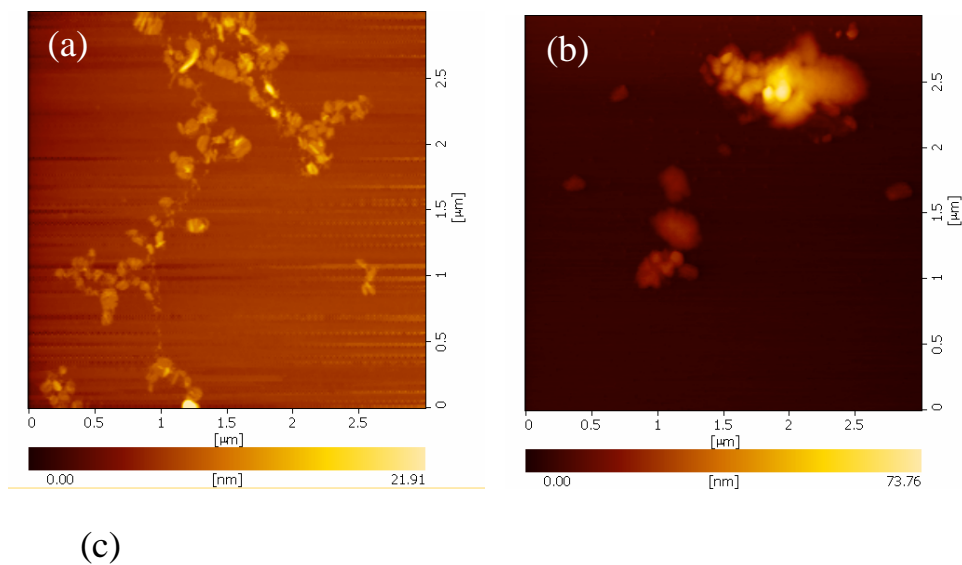


Figure 3.13 AFM images of PDA vesicles obtained from air dry samples of 5EG-PCDA/PCDA (30/70% mole) mixed lipid sols on mica surface before (a) after an addition of $100 \mu\text{M Pb}^{2+}$ (b) size distribution by intensity of 30% 5EG-PCDA/PCDA before (red) and after (green) addition of $100 \mu\text{M Pb}^{2+}$ (c) and the proposed mechanism for the Pb^{2+} induced color transition (d).

The dynamic range of 5EG-PCDA/PCDA (30/70% mol) sol for Pb^{2+} detection was determined by varying the solution of $\text{Pb}(\text{NO}_3)_2$ concentration from 5 to 100 μM . Linear colorimetric response was obtained with Pb^{2+} concentration in the range of 5-30 μM (**Figure 3.14**). Noticeable color change with %CR of 20% was observed with the concentration of Pb^{2+} as low as 10 μM (~2 ppm). As the second most sensitive ion, Zn^{2+} showed low %CR of less than 20% up to 100 μM . Importantly, no color change was observed in the presence of alkaline and alkaline earth metal ions such as Li^+ , Na^+ , K^+ , Ca^{2+} , and Mg^{2+} at 100 μM concentration (**Figure 3.15**) indicating that there is no interference from such metal ions to this PDA sensor system.

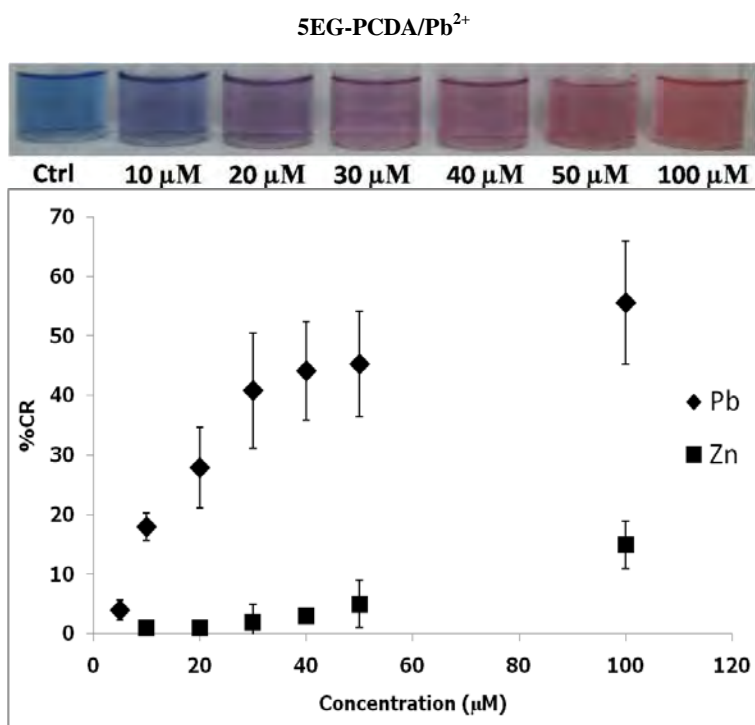


Figure 3.14 Colorimetric responses (%CR) to various concentration Pb^{2+} and Zn^{2+} of the PDA sol (0.1 mM) prepared from PCDA mixed with 30% mole of 5EG-PCDA. The picture at the top shows visual appearance of the sols upon the addition of Pb^{2+} ion at the corresponding concentrations.

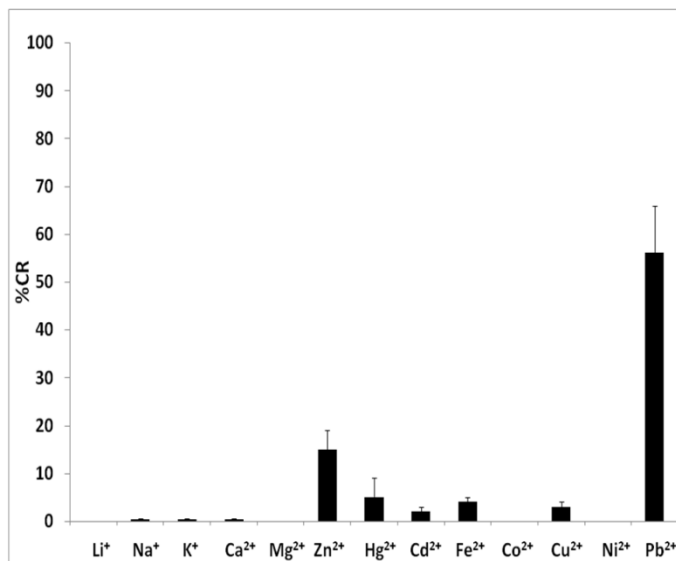
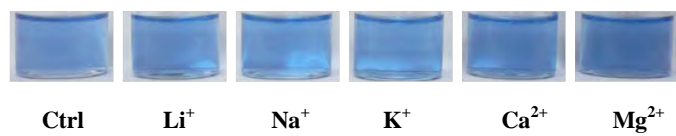


Figure 3.15 Colorimetric responses (%CR) to various metal ions (100 μ M) of the mixed lipid PDA sols of 5EG-PCDA/PCDA (30/70% mole).

CHAPTER IV

CONCLUSION

The polydiacetylene sols prepared from 10,12-pentacosadiynoic acid (PCDA) and its oligo(ethylene glycol) esters derived from ethylene glycol (EG), triethylene glycol (3EG) and pentaethylene glycol (5EG) were successfully synthesized. The glycol ester lipids were hydrated and well dispersed in water but they did not polymerize upon UV irradiation suggesting some sort of loose packing within their molecular self-assembly. They however could be mixed with PCDA up to 30% mole and polymerized to form homogeneous blue sols. These mixed lipid sols showed blue to red color transition with two-stepped transition temperatures. The first transition temperature decreased with the increasing content of the glycol ester lipid and length of the ethylene glycol chains while the second transition temperature was observed at essentially the same as that of poly(PCDA). The thermochromic results indicated that the incorporation of the ethylene glycol chain increased the fluidity of the self-assembled structure by lessening the collaborative hydrogen bonding among the lipid head groups. Furthermore, the mixed polydiacetylene sols also exhibited selective colorimetric blue-red response to Pb^{2+} ion while the unmodified poly(PCDA) sol did not. The most sensitive polydiacetylene sols contained 30 mol% of 5EG-PCDA that could be detected by naked eye at part per million levels; 10 μM or 2 ppm of Pb^{2+} gave 20 %CR. The atomic force microscopic image revealed that Pb^{2+} induced aggregation and rupture of the PDA vesicles. The Pb^{2+} probably bound to the carboxylic/carboxylate groups on the vesicle surface inducing the deformation of the lipid bi-layered membrane in which its fluidity enhanced by the incorporation of the oligo(ethylene glycol) lipid.

REFERENCES

- [1] Lim, C.; Sandman, D. J.; Sukwattanasinitt, M. Topological polymerization of tert-Butylcalix[4]arenes containing diynes, Macromolecules 41 (2008) 675–681.
- [2] Lim, C.; Sandman, D. J.; Sukwattanasinitt, M.; Foxman, B. M. Synthesis and crystallographic study of 1,6-bis-(N-phenothiazinyl)-2,4-hexadiyne, J. Macromol. Sci., Part A: Pure Appl. Chem. 43 (2006) 1929–1936.
- [3] Nadizadeh, H.; Mattern, D. L. Langmuir-blodgett films of donor- π -acceptor (D- π -A) compounds, where D = anilide donors with internal diyne or saturated lipid tails, π = carbamate bridge, and A = 4-Nitrophenyl or TCNQ acceptors, Chem. Mater. 6 (1994) 268–277.
- [4] Baughman, R. H.; Yee, K. C. Solid-state polymerization of linear and cyclic acetylenes, J. Polym. Sci., Part D: Macromol. Rev. 13 (1978) 219-239.
- [5] Enkelmann, V. Structural aspects of the topochemical polymerization of diacetylenes, Adv. Polym. Sci. 63 (1984) 91-136.
- [6] Reichert, A.; Nagy, J. O.; Spevak, W.; Charych, D. H. Polydiacetylene liposomes functionalized with sialic acid bind and colorimetrically detect influenza virus, J. Am. Chem. Soc. 117 (1995) 829–830.
- [7] Deng, J.; Sheng, Z.; Zhou, K.; Duan, M.; Yu, C. Y.; Jiang, L. Construction of effective receptor for recognition of avian influenza H5N1 Protein HA1 by Assembly of monohead glycolipids on polydiacetylene vesicle surface, Bioconjugate Chem. 20 (2009) 533–537.
- [8] Reppy, M.A.; Pindzola, B.A. Biosensing with polydiacetylene materials: structures, optical properties and applications, Chem. Commun. (2007) 4137–4338.
- [9] Ma, G.; Cheng, Q. Vesicular polydiacetylene sensor for colorimetric signaling of bacterial pore-forming toxin, Langmuir 21 (2005) 6123–6126.
- [10] Kolusheva, S.; Kafri, R.; Katz, M.; Jelinek, R. Rapid colorimetric detection of antibody-epitope recognition at a biomimetic membrane interface, J. Am. Chem. Soc. 123 (2001) 417–422.

- [11] Kolusheva, S.; Shahal, T.; Jelinek, R. Peptide-membrane interactions studied by a new phospholipid/polydiacetylene colorimetric vesicle assay, Biochemistry 39 (2000) 15851–15859.
- [12] Pan, J. J.; Charych, D. Molecular recognition and colorimetric detection of Cholera toxin by poly(diacetylene) liposomes incorporating Gm1 ganglioside, Langmuir 13 (1997) 1365–1367.
- [13] Charych, D and others A litmus test for molecular recognition using artificial membranes, Chem. Biol. 3 (1996) 113–120.
- [14] Charych, D. H.; Nagy, J. O.; Spevak, W.; Bednarski, M. D. Direct colorimetric detection of a receptor-ligand interaction by a polymerized bilayer assembly, Science 261 (1993) 585–588.
- [15] Champaiboon, T.; Tumcharern, G.; Potisatityuenyong, A.; Wacharasindhu, S.; Sukwattanasinitt, M. A polydiacetylene multilayer film for naked eye detection of aromatic compounds, Sens. Actuator B-Chem. 139 (2009) 532–537.
- [16] Yoon, J.; Chae, S.; Kim, J. Colorimetric sensors for volatile organic compounds (VOCs) based on conjugated polymer-embedded electrospun fibers, J. Am. Chem. Soc. 129 (2007) 3038–3039.
- [17] Ahn, D. J.; Kim, J. M. Fluorogenic polydiacetylene supramolecules: immobilization, micropatterning, and application to Label-Free chemosensors, Acc. Chem. Res. 41 (2008) 805–816.
- [18] Kolusheva, S.; Shahal, T.; Jelinek, R. Cation-selective color sensors composed of ionophore-phospholipid-polydiacetylene mixed vesicles, J. Am. Chem. Soc. 122 (2000) 776–780.
- [19] Jose, D. A.; König, B. Polydiacetylene vesicles functionalized with *N*-heterocyclic ligands for metal cation binding, Org. Biomol. Chem. 8 (2010) 655–662.
- [20] Schott, M. The colors of polydiacetylenes: a commentary, J. Phys. Chem. B 110 (2006) 15864–15868.
- [21] Dobrosavljevic, V.; Stratt, R. M. The role of conformational disorder in the electronic structure of conjugated polymers: Substituted polydiacetylenes Phys. Rev. B 35 (1987) 2781–2794.

- [22] Dautel, O. J.; Robitzer, M.; Le` re-Porte, J. P.; Serein-Spirau, F.; Moreau, J. L. Self-organized ureido substituted diacetylenic organogel. photopolymerization of one-dimensional supramolecular assemblies to give conjugated nanofibers, J. Am. Chem. Soc. 128 (2006) 16213-16223.
- [23] Fujita, N.; Sakamoto, Y.; Shirakawa, M.; Ojima, M.; Fuji, A.; Ozaki, M.; Shinkai, Seiji. Polydiacetylene nanofibers created in low-molecular-weight gels by post modification: control of blue and red phases by odd-even effect in alkyl chains, J. Am. Chem. Soc. 129 (2007) 4134-4135.
- [24] Potisatityuenyong, A.; Rojanathanes, R.; Tumcharern, G.; Sukwattanasinitt, M. Electronic absorption spectroscopy probed side-chain movement in chromic transitions of polydiacetylene vesicles, Langmuir 24 (2008) 4461-4463.
- [25] Dei, S.; Shingaki, T.; Matsumoto, A. Thermochromism of polydiacetylene containing robust 2D hydrogen bond network of naphthylmethylammonium carboxylates, Macromolecules 41 (2008) 6055-6065.
- [26] Wan, X.; Sandman, D. J. Thermochromic polydiacetylene micro- and nanocrystals: an unusual size effect in electronic spectra, Macromolecules 41 (2008) 773-778.
- [27] Kim, J. M.; Lee, J. S.; Choi, H.; Solin, D.; Ahn, D. J.; Rational design and in-situ FTIR Analyses of colorimetrically reversible polydiacetylene supramolecules, Macromolecules 38 (2005) 9366-9376.
- [28] Carpick, R. W.; Mayer, T. M.; Sasaki, D. Y.; Burns, A. R. Spectroscopic ellipsometry and fluorescence study of thermochromism in an ultrathin polydiacetylene film: reversibility and transition kinetics, Langmuir 16 (2000) 4639-4647.
- [29] Hua, Q.; Russell, K.C.; Leblanc, R. M. Chromatic studies of a polymerizable diacetylene hydrogen bonding self-assembly: a self-folding process to explain the chromatic changes of polydiacetylenes, Langmuir 15 (1999) 3972-3980.

- [30] Beckham, H. W.; Rubner, M. F. On the origin of thermochromism in cross-polymerized diacetylene-functionalized polyamides, Macromolecules 26 (1993) 5198-5201.
- [31] Exarhos, G. J.; Risen, Jr., W. M.; Baughman, R. H. Resonance Raman study of the thermochromic phase transition of a polydiacetylene, J. Am. Chem. Soc. 98 (1976) 481-487.
- [32] Chance, R. R. Chromism in polydiacetylene solutions and crystals Macromolecules 13 (1980) 396-398.
- [33] Nallicheri, R. A.; Rubner, M. F. Investigations of the mechanochromic behavior of poly(urethane diacetylene) segmented copolymers, Macromolecules 24 (1991) 517-525.
- [34] Gu, Y.; Cao, W.; Zhu, L.; Chen, D.; Jiang, M.; Polymer mortar assisted self-assembly of nanocrystalline polydiacetylene bricks showing reversible thermochromism Macromolecules 41 (2008) 2299-2303.
- [35] Wacharasindhu, S.; Montha, S.; Boonyiseng, J.; Potisatiyuenyong, A.; Phollookin, C.; Tumcharern, G.; Sukwattanasinitt, M. Tuning of thermochromic properties of polydiacetylene toward universal temperature sensing materials through amido hydrogen bonding, Macromolecules 43 (2010) 716-724.
- [36] Muller, H.; Eckhardt, C.J. Stress induced change of electronic structure in a polydiacetylene crystal, Mol. Cryst. Liq. Cryst. 45 (1978) 313-318.
- [37] Lee, J.; Kim, H. J.; Kim, J. Polydiacetylene liposome arrays for selective potassium detection, J. Am. Chem. Soc. 130 (2008) 5010-5011.
- [38] Sasaki, D.Y.; Waggoner, T.A.; Last, J.A.; Alam, T.M. Crown ether functionalized lipid membranes: Lead ion recognition and molecular reorganization, Langmuir 18 (2002) 3714-3721.
- [39] Pincus, J.L.; Jin, C.; Huang, W.; Jacobs, H.K.; Gopalan, A.S.; Song, Y.; Shelnut, J.A.; Sasaki, D.Y. Selective fluorescence detection of divalent and trivalent metal ions with functionalized lipid membranes, J. Mater. Chem. 15 (2005) 2938-2945.

- [40] Waggoner, T.A.; Last, J.A.; Kotula, P.G.; Sasaki, D.Y. Self-assembled columns of stacked lipid bilayers mediated by metal ion recognition, J. Am. Chem. Soc. 123 (2001) 496-497.
- [41] Yin, X.; Stover, H. D. H. Thermosensitive and pH-sensitive polymers based on maleic anhydride copolymers, Macromolecules 35 (2002) 10178–10181.
- [42] Zhao, B.; Li, D.; Hua, F.; Green, D. R.; Synthesis of Thermosensitive Water-Soluble Polystyrenics with Pendant Methoxyoligo(ethylene glycol) Groups by Nitroxide-Mediated Radical Polymerization, Macromolecules 38 (2005) 9509-9517
- [43] Li, D. Jones, G. L.; Dunlap, J. R.; Hua, F.; Zhao, B. Thermosensitive hairy hybrid nanoparticles synthesized by surface-initiated atom transfer radical polymerization, Langmuir 22 (2006) 3344–3351.
- [44] Saha, A.; Ramakrishnan, S. AB₂ + A type copolymerization approach for the preparation of thermosensitive PEGylated hyperbranched polymers, Macromolecules 41 (2008) 5658–5644.
- [45] Frech, R.; Huang, W. Conformational changes in diethylene glycol dimethyl ether and poly(ethylene oxide) induced by lithium ion complexation, Macromolecules 28 (1995) 1246–1251.
- [46] Liu, C. W.; Huang, C. C.; Chang, H. T Highly selective DNA-based sensor for lead(II) and mercury(II) ions, Anal. Chem. 81 (2009) 2383-2387.
- [47] Xiang, Y.; Tong, A.; Lu, Yi. Abasic site-containing DNzyme and Aptamer for label-free fluorescent detection of Pb and adenosine with high sensitivity, selectivity, and tunable dynamic range, J. Am. Chem. Soc. 131 (2009) 15352–15357.
- [48] Wang, H.; Kim, Y.; Liu, H.; Zhu, Z.; Bamrungsap, S.; Tan, W. Engineering a unimolecular DNA-catalytic probe for single lead ion monitoring, J. Am. Chem. Soc. 131 (2009) 8221–8226.
- [49] Zapata, F.; Caballero, A.; Espinosa, A.; Tárraga, A.; Molina, P. Triple channel sensing of Pb ions by a simple multiresponsive ferrocene receptor having a 1-deazapurine backbone, Org. Lett. 10 (2008) 41–44.

- [50] Guo, L.; Hong, S.; Lin, X.; Xie, Z.; Chen, G. An organically modified sol-gel membrane for detection of lead ion by using 2-hydroxy-1-naphthaldehyde-8-aminoquinoline as fluorescence probe, Sens. Actuator B-Chem. 130 (2008) 789–794
- [51] Kavllieratos, K.; Rosenberg, J. M.; Chen, W. Z.; Ren, T. Fluorescent sensing and selective Pb extraction by a dansylamide ion-exchanger, J. Am. Chem. Soc. 127 (2005) 6514–6515.
- [52] Change, I. H.; Tulock, J. J.; Liu, J.; Kim, W. S.; Cannon, Jr., D. M.; Lu, Y.; Bohn, P. W.; Sweedler, J. V.; Cropek, D. M. Miniaturized lead sensor based on lead-specific DNAzyme in a nanocapillary interconnected microfluidic device, Environ. Sci. Technol. 39 (2005) 3756–3761.
- [53] Ma, L.; Li, H.; Wua, Y. A pyrene-containing fluorescent sensor with high selectivity for lead(II) ion in water with dual illustration of ground-state dimer, Sens. Actuator B-Chem. 143 (2009) 25–29
- [54] Kumar, M.; Babu, J. N.; Bhalla, V.; Kumar, R. Ratiometric on-off sensing of Pb²⁺ ion using pyrene-appended calix[4]arenes, Sens. Actuator B-Chem. 144 (2010) 183–191
- [55] Wang, J.; Chu, S.; Kong, F.; Luo, L.; Wang, Y.; Zou, Z. Designing a smart fluorescence chemosensor within the tailored channel of mesoporous material for sensitively monitoring toxic heavy metal ions Pb (II), Sens. Actuator B-Chem.: Chemical (2010), doi:10.1016/j.snb.2010.07.050
- [56] Li, T.; Wang, E.; Dong, S. Lead(II)-induced allosteric G-quadruplex DNAzyme as a colorimetric and chemiluminescence sensor for highly sensitive and selective Pb detection, Anal. Chem. 82 (2010) 1515–1520.
- [57] Chen, Y. Y.; Chang, H. T.; Shiang, Y. C.; Hung, Y. L.; Chiang, C. K.; Huang, C. C. Colorimetric assay for lead ions based on the leaching of gold nanoparticles, Anal. Chem. 81 (2009) 9433–9439.
- [58] Liu, J.; Lu, Y. Optimization of a Pb²⁺ directed gold nanoparticle/DNAzyme assembly and its application as a colorimetric biosensor for Pb²⁺, Chem. Mater. 16 (2004) 3231–328.

- [59] Liu, J.; Lu, Y. Accelerated color change of gold nanoparticles assembled by DNAzymes for simple and fast colorimetric Pb detection, J. Am. Chem. Soc. 126 (2004) 12298–12305.
- [60] Liu, J.; Lu, Y. A colorimetric lead biosensor using DNAzyme-directed assembly of gold nanoparticles, J. Am. Chem. Soc. 125 (2003) 6642–6643.
- [61] Shen, L.; Chen, Z.; Li, Y.; He, S.; Xie, S.; Xu, X.; Liang, Z.; Meng, X.; Li, Q.; Zhu, Z.; Li, M.; Le, X. C.; Shao, Y. Electrochemical DNAzyme sensor for lead based on amplification of DNA-Au bio-bar codes, Anal. Chem. 80 (2008) 6323-6328.
- [62] Wilson, R.; Schiffrin, D.J.; Luff, B.J.; Wilkinson, J.S. Optoelectrochemical sensor for lead based on electrochemically assisted solvent extraction, Sens. Actuator B-Chem. 63 (2000) 115–121
- [63] Mousavi, M.F.; Barzegar, M.B.; Sahari, S. A PVC-based capric acid membrane potentiometric sensor for lead(II) ions, Sens. Actuator B-Chem. 73 (2001) 199–204
- [64] Mazloum Ardakani, M.; Khayat Kashani, M.; Salavati-Niasari, M.; Ensafi, A.A. Lead ion-selective electrode prepared by sol–gel and PVC membrane techniques, Sens. Actuator B-Chem. 107 (2005) 438–445
- [65] Senthilkumar, S.; Saraswathi, R.; Electrochemical sensing of cadmium and lead ions at zeolite-modified electrodes: optimization and field measurements, Sens. Actuator B-Chem. 141 (2009) 65–75.
- [66] Deo, S.; Godwin, H. A. A Selective, Ratiometric Fluorescent Sensor for Pb²⁺, J. Am. Chem. Soc. 122 (2000) 174-175
- [67] Kwon, J. Y.; Jang, Y. J.; Lee, Y. J.; Kim, K. M.; Seo, M. S.; Nam, W.; Yoon, J. A Highly Selective Fluorescent Chemosensor for Pb²⁺, J. Am. Chem. Soc. 127 (2005) 10107-10111
- [68] Xiao, Y.; Rowe, A. A.; Plaxco, K. W. Electrochemical Detection of Parts-Per-Billion Lead via an Electrode-Bound DNAzyme Assembly, J. Am. Chem. Soc. 129 (2007) 262-263

- [69] Demeter, D.; Blanchard, P.; Allain, M.; Grosu, I.; Roncali, J. Synthesis and Metal Cation Complexing Properties of Crown-Annulated Terthiophenes Containing 3,4-Ethylene dioxythiophene, J. Org. Chem. 72 (2007) 5285-5290
- [70] Kim, J. W.; Lee, C. H.; Yoo, H. O.; Kim, J. M. Thermochromic polydiacetylene supramolecules with Oligo(ethyleneoxide) headgroups for tunable colorimetric response, Macromolecular Research 17 (2009) 441–444.
- [71] Hobbs, S.K.; Shi, G.; Bednarski, M. D. Synthesis of polymerized thin films for immobilized ligand display in proteomic analysis, Bioconjugate Chem. 14 (2003) 526–531.
- [72] Wilson, T. E.; Spevak, W.; Charych, D. H.; Bednarski, M. D. Enzymatic modification and X-ray photoelectron spectroscopy analysis of a functionalized polydiacetylene thin film, Langmuir 10(1994) 1512–1516.
- [73] Wilson, T. E.; Bednarski, M. D. Polydiacetylene monolayers functionalized with amino acids, Langmuir 8 (1992) 2361–2364.

APPENDICES

APPENDIX A
NMR SPECTRA

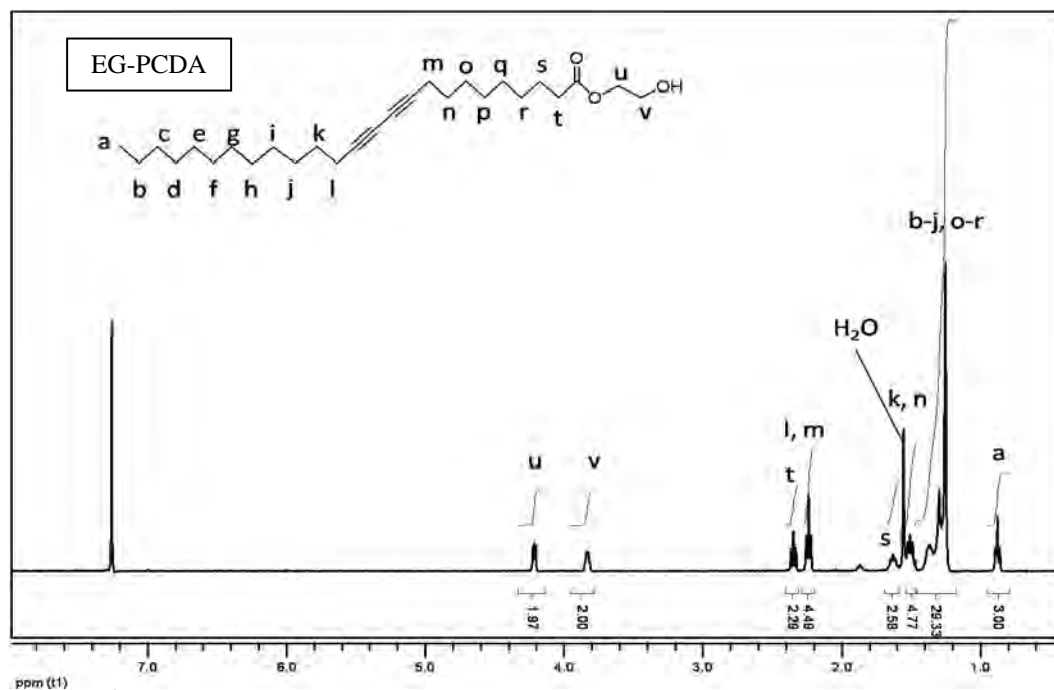


Figure A1 ¹H NMR; 2-hydroxyethyl pentacos-10,12-dienoate (EG-PCDA).

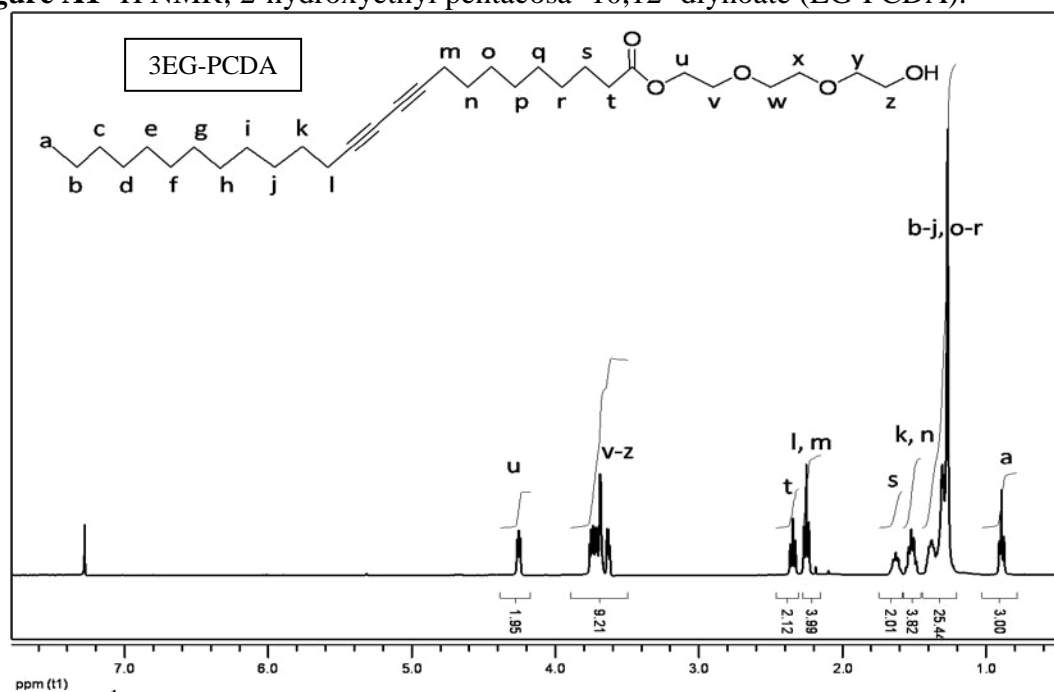


Figure A2 ¹H NMR; 2-(2-(2 hydroxyethoxy) ethoxy) ethyl pentacos-10,12-dienoate (3EG-PCDA)

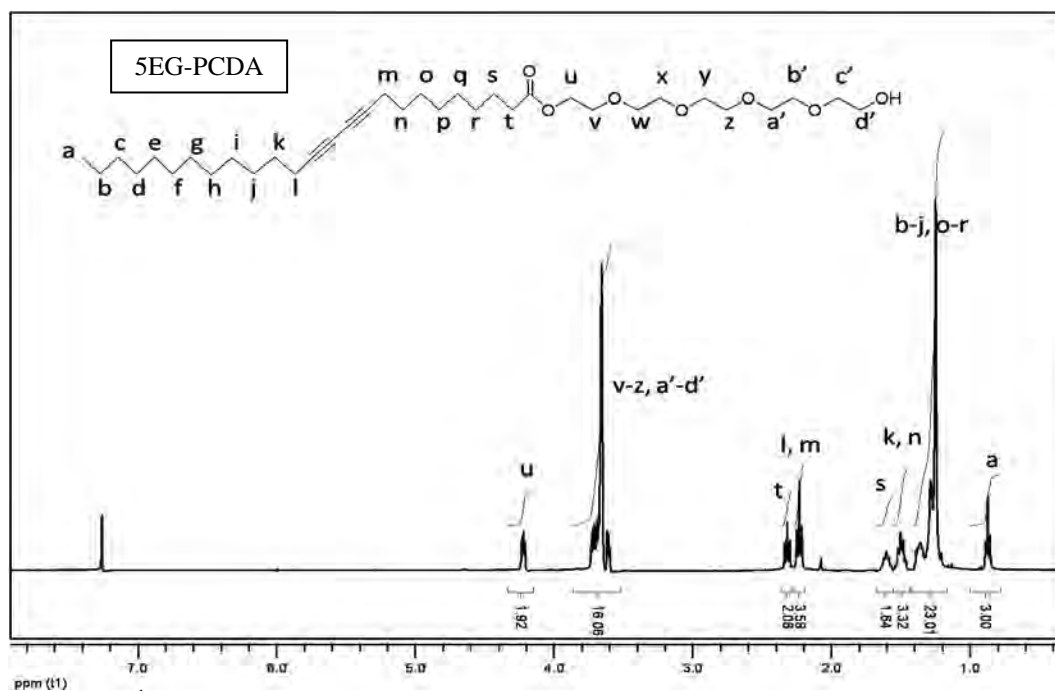


Figure A3 ^1H NMR; 14-hydroxy-3,6,9,12-tetraoxatetradecyl pentacos-10,12-diyanoate (5EG-PCDA).

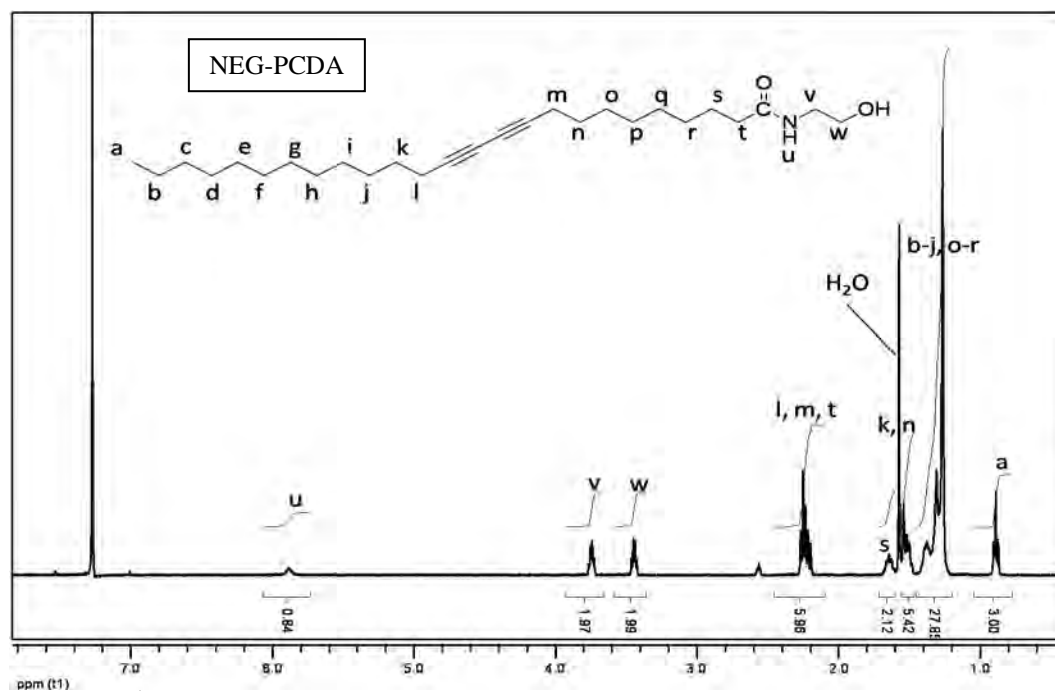


Figure A4 ^1H NMR; N-(2-hydroxyethyl) pentacos-10,12-diynamide (NEG-PCDA)

Figure A5 ^{13}C NMR; 2-hydroxyethyl pentacos- 10,12- diynoate (EG-PCDA).

Figure A6 ^{13}C NMR; 2-(2-(2 hydroxyethoxy) ethoxy) ethyl pentacos-10,12-diynoate (3EG-PCDA)

Figure A7 ^{13}C NMR; 14-hydroxy-3,6,9,12-tetraoxatetradecyl pentacos-10,12-dienoate (5EG-PCDA).

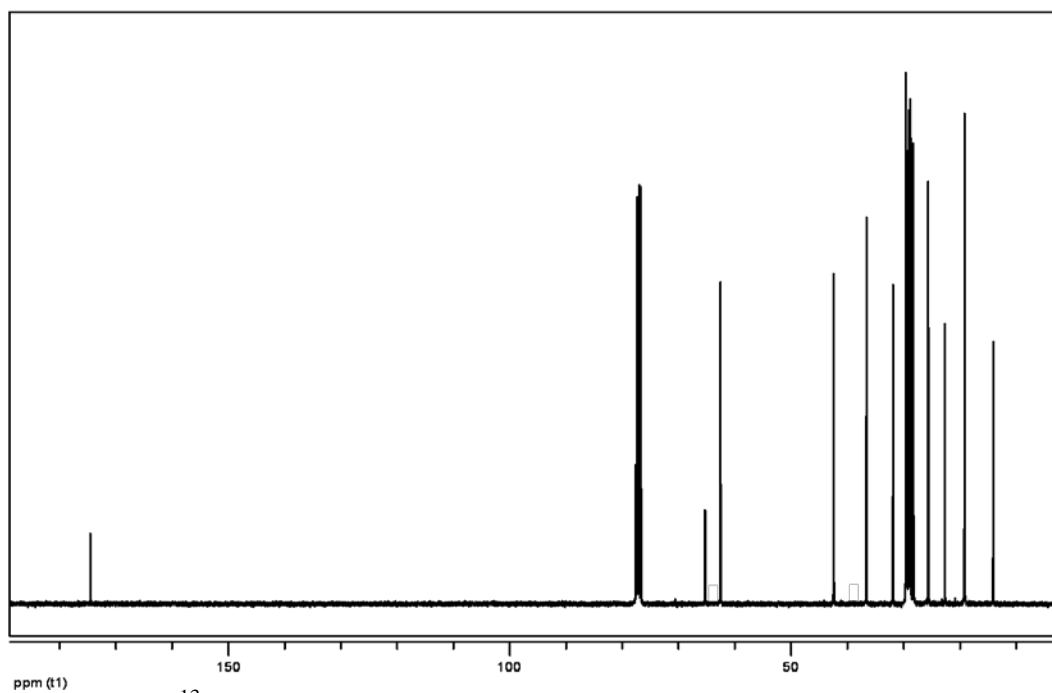


Figure A8 ^{13}C NMR; N-(2hydroxyethyl) pentacos-10,12-diynamide (NEG-PCDA)

APPENDIX B MASS SPECTRA

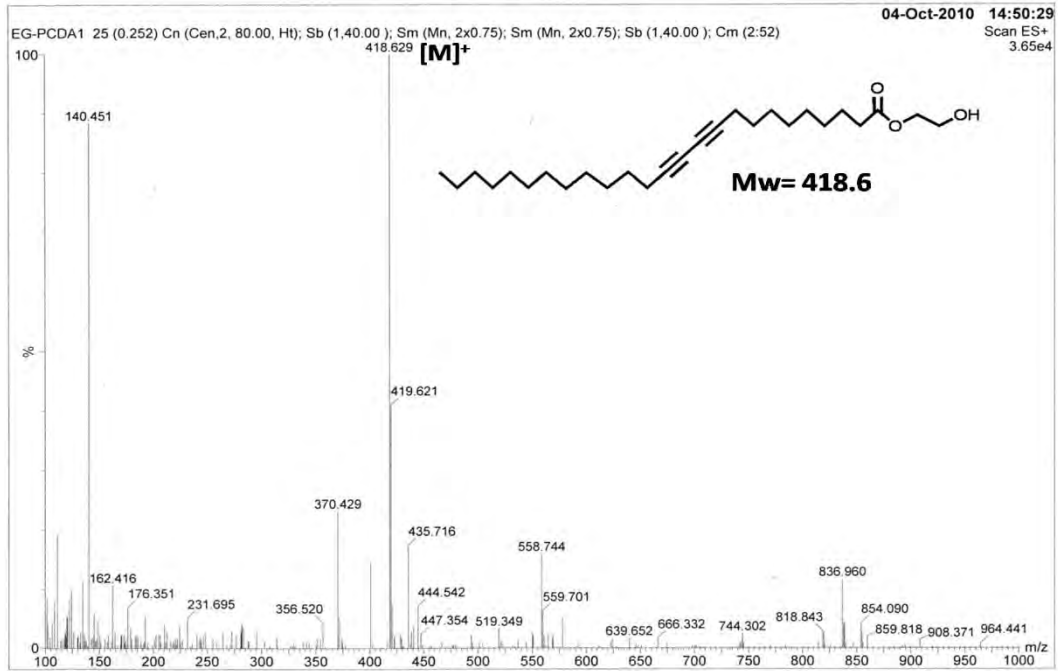


Figure B1 Mass spectra(ESI+) of EG-PCDA

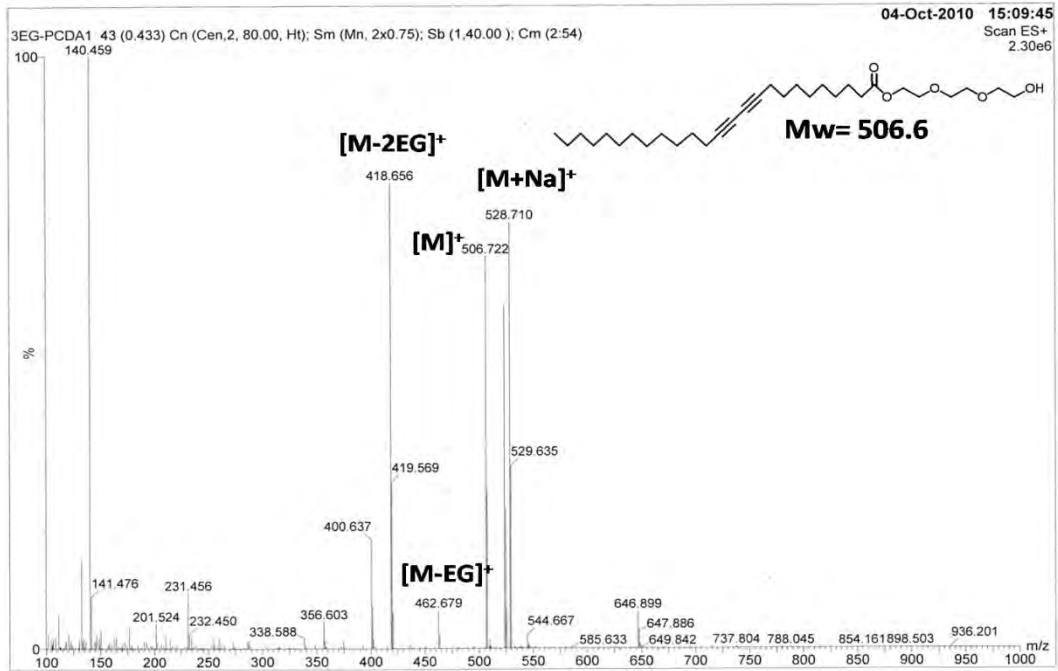


Figure B2 Mass spectra(ESI+) of 3EG-PCDA



Figure B3 Mass spectra(ESI+) of 5EG-PCDA

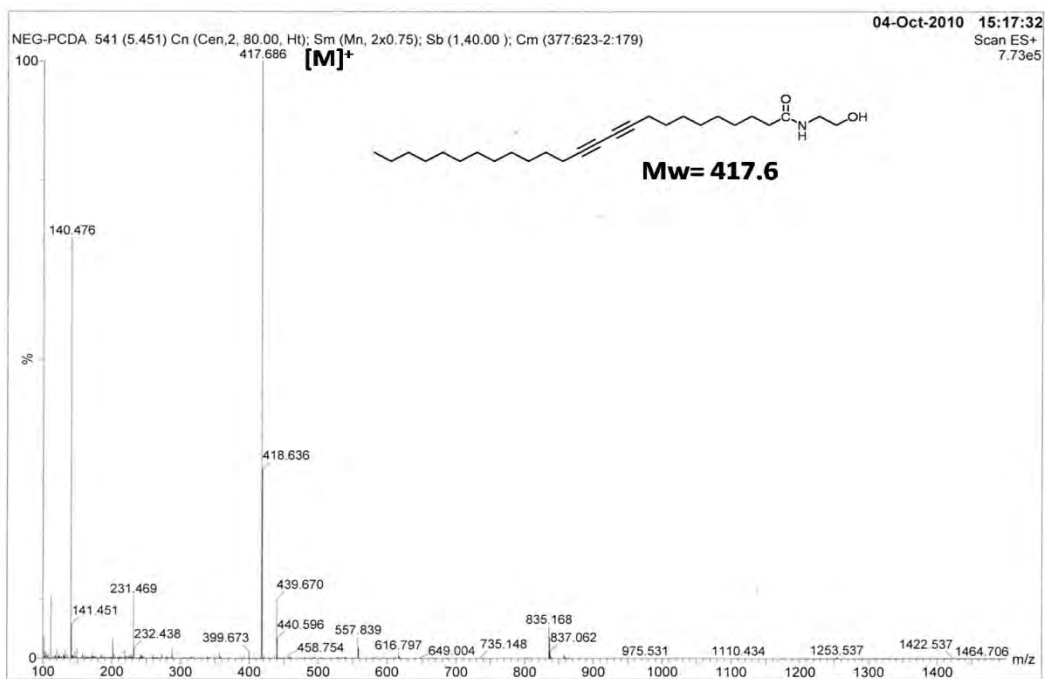


Figure B4 Mass spectra(ESI+) of NEG-PCDA

APPENDIX C UV-VISIBLE ABSORPTION SPECTRA

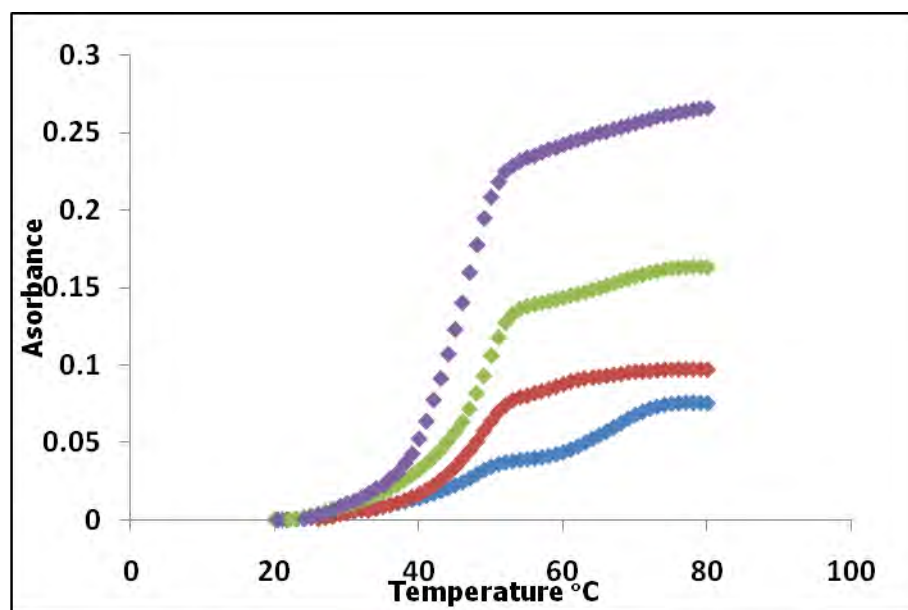


Figure C1 Temperature dependence of the absorbance (A) at 540 nm of the mixed lipid sols EG-PCDA/PCDA 10% ■; 20% ■; 30% ■; 50% ■.

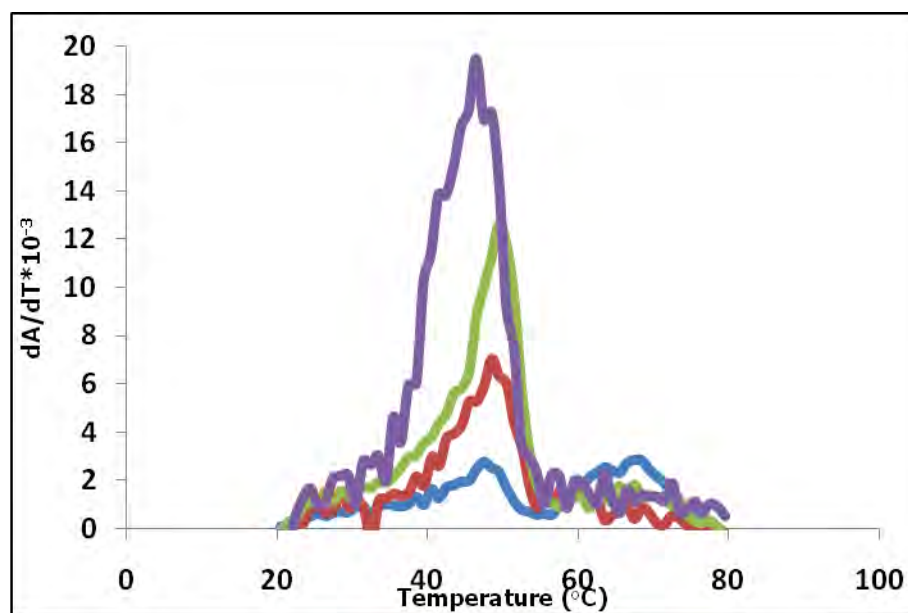


Figure C2 Derivative plot (dA/dT) of mixed lipid sols EG-PCDA/PCDA 10% ■; 20% ■; 30% ■; 50% ■.

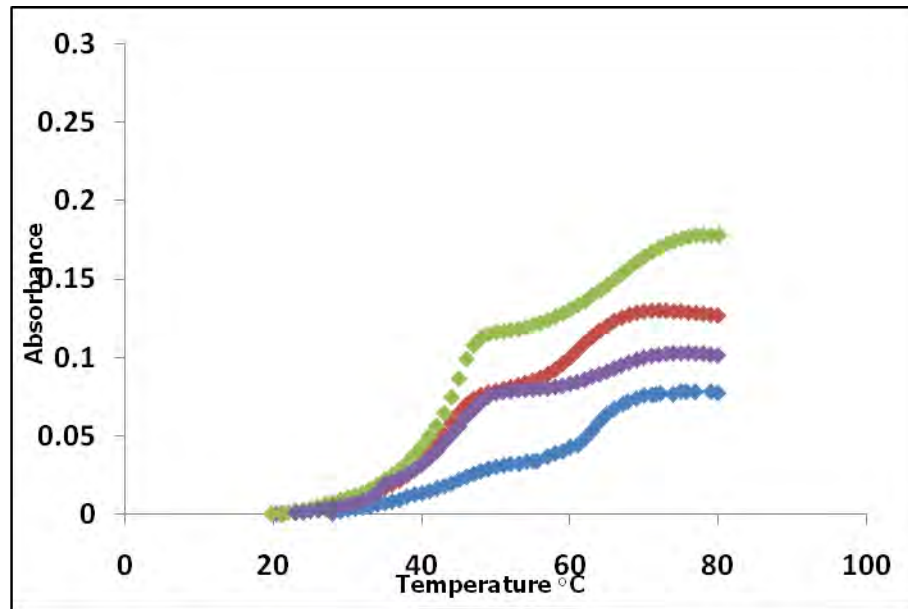


Figure C3 Temperature dependence of the absorbance (A) at 540 nm of the mixed lipid sols 3EG-PCDA/PCDA 10% ■; 20% ■; 30% ■; 50% ■.

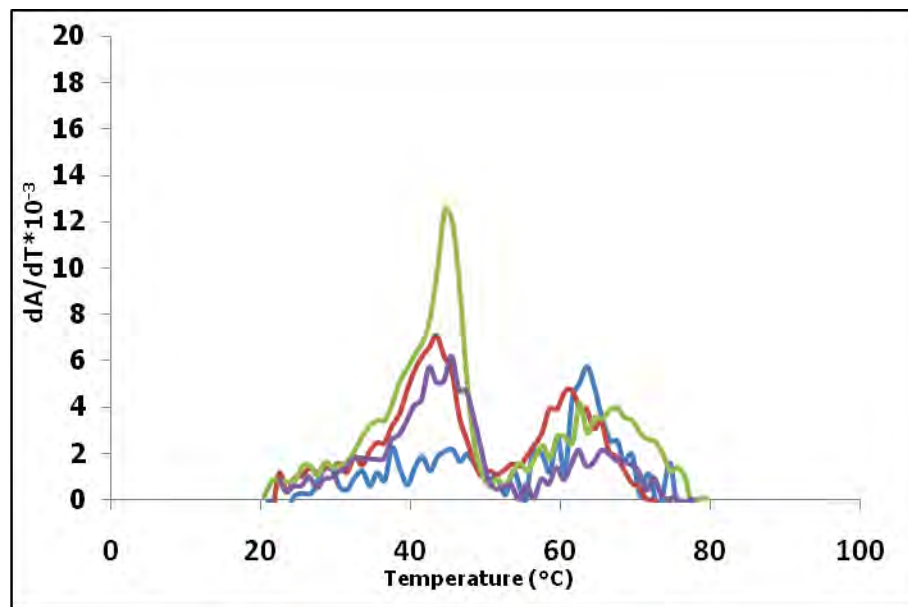


Figure C4 Derivative plot (dA/dT) of mixed lipid sols 3EG-PCDA/PCDA 10% ■; 20% ■; 30% ■; 50% ■.

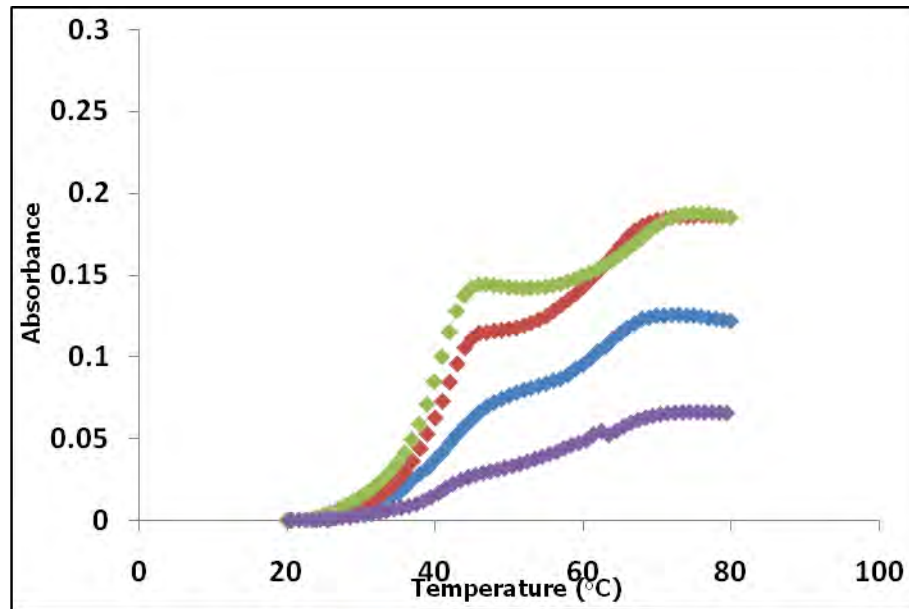


Figure C5 Temperature dependence of the absorbance (A) at 540 nm of the mixed lipid sols 5EG-PCDA/PCDA 10% ■; 20% ■; 30% ■; 50% ■.

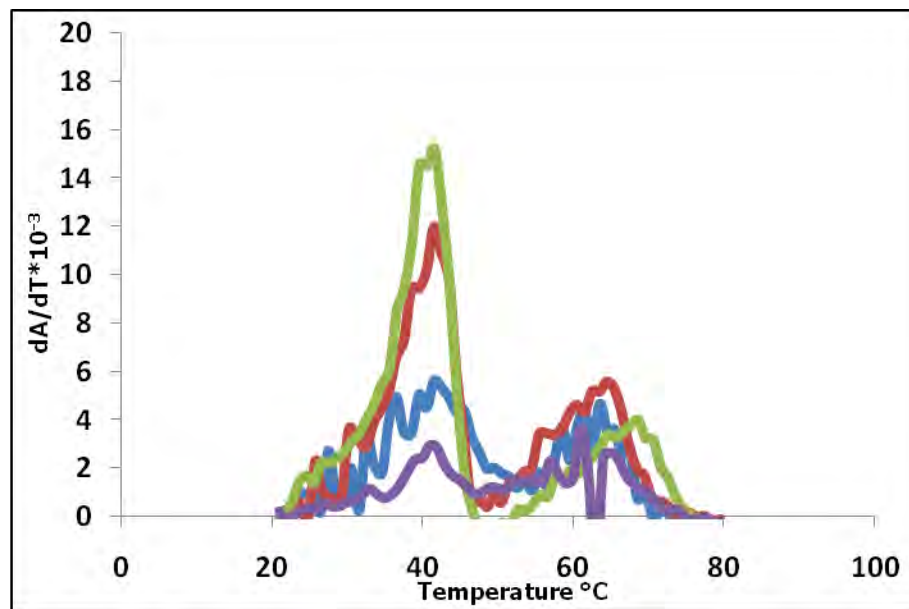


Figure C6 Derivative plot (dA/dT) of mixed lipid sols 5EG-PCDA/PCDA 10% ■; 20% ■; 30% ■; 50% ■.

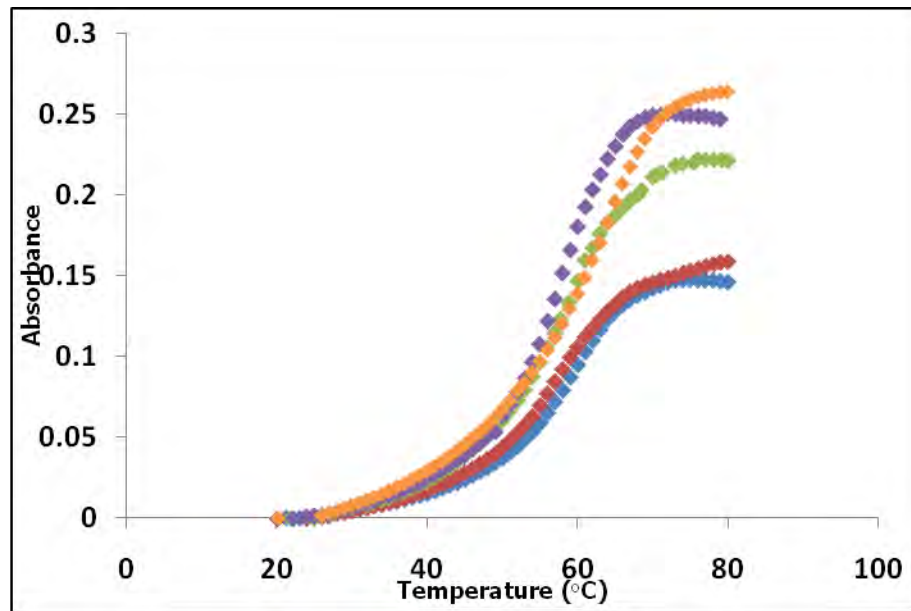


Figure C7 Temperature dependence of the absorbance (A) at 540 nm of the mixed lipid sols NEG-PCDA/PCDA 10% ■; 20% ■; 30% ■; 50% ■; 100% ■.

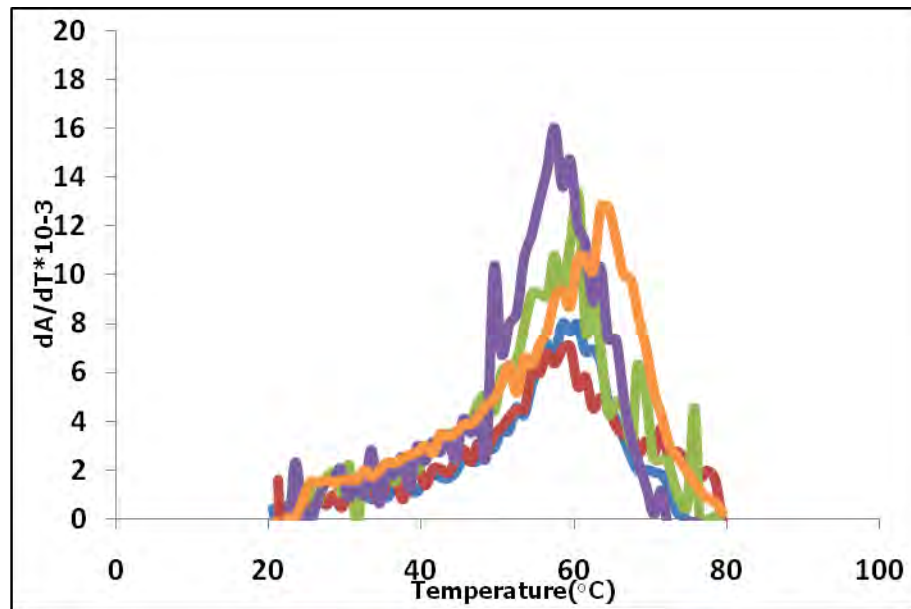


Figure C8 Derivative plot (dA/dT) of mixed lipid sols NEG-PCDA/PCDA 10% ■; 20% ■; 30% ■; 50% ■; 100% ■.

VITAE

Pat Narkwiboonwong was born on August 12st, 1984 in Bangkok, Thailand. He received a Bachelor's Degree of Science, majoring in Chemistry from Faculty of Science, Naresuan University in 2006. Since 2007, he has been a graduate student studying Petrochemistry and Polymer Science as his major course from Faculty of Science, Chulalongkorn University and completed the program in academic year of 2010.

His present address is 8/118 Phetkasem Bangduan Phasicahreern Bangkok, Thailand 10110.